Determining 3D Relative Transformations for Any Combination of Range and Bearing Measurements

Xun S. Zhou and Stergios I. Roumeliotis

***Abstract*—In this paper, we address the problem of motion-induced 3D robot-to-robot extrinsic calibration based on ego-motion estimates and combinations of inter-robot measurements (i.e., distance and/or bearing observations from either or both of the two robots, recorded across multiple time steps). In particular, we focus on solving *minimal* problems where the unknown 6-degrees-of-freedom (DOF) transformation between the two robots is determined based on the minimum number of measurements necessary for finding a finite set of solutions. In order to address the very large number of possible combinations of inter-robot observations, we identify symmetries in the measurement sequence and use them to prove that any extrinsic robot-to-robot calibration problem can be solved based on the solutions of only 14 (base) minimal problems. Moreover, we provide algebraic (closed-form) and efficient symbolic-numerical (analytical) solution methods to these minimal problems. Finally, we evaluate the performance of our proposed solvers through extensive simulations and experiments.**

I. Introduction

Multi-robot systems have attracted considerable attention due to their wide range of applications, such as search and rescue [1], target tracking [2], cooperative localization [3], and mapping [4]. In order to accomplish these tasks cooperatively, it is necessary for the robots to share their sensor measurements. These measurements, however, are registered with respect to each robot's local reference frame and need to be converted to a common reference frame before they can be fused. Such a conversion requires knowledge of the robot-to-robot transformation, i.e., their relative position and orientation (pose). Most multi-robot estimation algorithms assume that this robot-to-robot transformation is known. However, only few works describe how to compute it.

The 6-DOF transformation between two robots can be determined by *manually* measuring their relative pose. This approach, however, has several drawbacks: it is tedious and time consuming, it often has limited accuracy, and it is inefficient when considering large robot teams. An alternative method is to use *external references* (e.g., GPS, compass, or a prior map of the environment). However, such references are not always available due to environment constraints (e.g., underwater, underground, outer space, or indoors).

In the absence of external references, the relative robot-to-robot transformation can be computed using *inter-robot observations*, i.e., robot-to-robot distance and/or bearing measurements. For example, for the case of a *static* sensor network, numerous methods have been proposed for determining the locations of the sensors using distance-only measurements between neighboring sensors (e.g., [5], [6]). However, these approaches are limited to estimating only the 2D *positions* of static sensors.

In order to estimate their 6-DOF transformation, the robots will have to move and collect multiple distance and bearing measurements to each other. Then their relative pose can be determined using: (i) the inter-robot observations and (ii) the robots' motion estimates. This task of *motion-induced extrinsic calibration* is precisely the problem addressed in this paper. When compared to alternative approaches that rely on external references, motion-induced calibration is more cost efficient since no additional hardware is required, and can be applied in unknown environments where no external aids are available. Additionally, recalibration can be easily carried out in the field when necessary.

In this paper, we focus on solving minimal systems where the number of equations provided by the inter-robot measurements equals the number of unknown parameters[1] [7], [8]. In particular, we consider the case where the robots are equipped with different types of sensors, or record different types of relative measurements over time due to environment constraints. Such minimal problems are formulated as systems of multivariate polynomial equations which, in general, have multiple (complex) solutions. Even though we are only interested in the unique solution that corresponds to the true relative pose, the minimal solvers are extremely useful in practice mainly for two reasons: (i) in the presence of measurement outliers, using minimal solvers as hypothesis generators minimizes the number of samples required in an outlier-rejection scheme such as Random Sample Consensus (RANSAC) [9], (ii) minimal solvers can be used to initialize an iterative process [e.g., nonlinear weighted least squares (NWLS)] for improving the estimation accuracy when additional measurements are available[2].

The solutions for each minimal problem are derived as if all measurements are noise-free. In this case, one of the solutions of the minimal problem is also a solution of an over-determined problem. However, in practice, the measurements are contaminated with noise. The effect of the measurement noise to the minimal solutions is evaluated by Monte Carlo simulations. In addition, when more than the minimal number

This work was supported by the Digital Technology Center (DTC), University of Minnesota, and the National Science Foundation (IIS-0811946).

Xun S. Zhou is with SRI International Sarnoff, Princeton, NJ; Stergios I. Roumeliotis is with the Department of Computer Science and Engineering, University of Minnesota, Minneapolis, MN, 55455 USA email: {zhou|stergios}@cs.umn.edu

[1] As compared to our recent conference publications [7] and [8], in this article we provide further derivations of the two singular cases (Systems 3 and 4), and improve the solution method of System 8, 9, and 10. Additionally, we have included experimental results for evaluating the performance of our solvers in practice.

[2] An additional advantage of NWLS is that it accounts for the effect of uncertainty and noise in the available motion estimates and inter-robot measurements, respectively.

of measurements are available, the solutions of the minimal problems are used to initialize a NWLS problem for minimizing the effect of noise.

The main contributions of this paper are twofold:

- We identify 14 base minimal systems and show that all other problems (including over-determined problems), resulting from different combinations of inter-robot measurements, can be solved using the solutions of the base systems.
- We determine the number of solutions of all the minimal systems, and provide closed-form and efficient symbolic-numerical (analytical) methods for solving them.

The remainder of the paper is structured as follows: After reviewing related work in Section II, we present the problem formulation and the 14 base minimal systems in Sections III and IV, respectively. The solution methodology for Systems 1 to 13 is described in Sections V to X. The accuracy of the presented methods is evaluated through extensive Monte-Carlo simulations in Section XI, and experiments in Section XII, followed by concluding remarks and future work in Section XIII.

II. Related Work

Previous work on *extrinsic calibration* of sensor networks using sensor-to-sensor range measurements, has primarily focused on *static* sensors in 2D with the limitation that only their *positions* are determined. Provided that a few anchor nodes can globally localize (e.g., via GPS), the global positions of the remaining nodes can be uniquely inferred if certain graph-rigidity constraints are satisfied [10], [11]. A variety of algorithms based on convex optimization [5], sum of squares (SOS) relaxation [12], and multi-dimensional scaling (MDS) [6] have been employed to localize the sensor nodes in 2D. In 3D, flying anchor nodes have been proposed to localize sensors, e.g., an aerial vehicle aiding static sensor network localization [13], or a single satellite localizing a stationary planetary rover [14]. However, all these methods only determine the *positions* of *static* sensors.

For many applications (e.g., localization, mapping, and tracking), knowledge of the sensors' relative position *and* orientation is required. However, using combinations of distance and bearing measurements to uniquely estimate relative poses in *static* 2D sensor networks was recently shown to be NP-hard [15]. For mobile sensors, the problem of relative pose determination has only been studied thoroughly in 2D. The ability to move and collect measurements from different vantage points provides additional information for localizing the sensors. This information has been shown to make the robots' relative pose observable, given inter-robot distance and/or bearing measurements [16]. Specifically, it is known that mutual distance *and* bearing measurements between two robots from a single vantage point are sufficient to determine the 3-DOF robot-to-robot transformation in closed-form [17], [18]. However, when only distance or bearing measurements are available, the robots must move and record additional observations. Then, the relative robot pose can be found by combining the estimated robot motions (e.g., from odometry) and the mutual bearing [16] or distance [19] measurements.

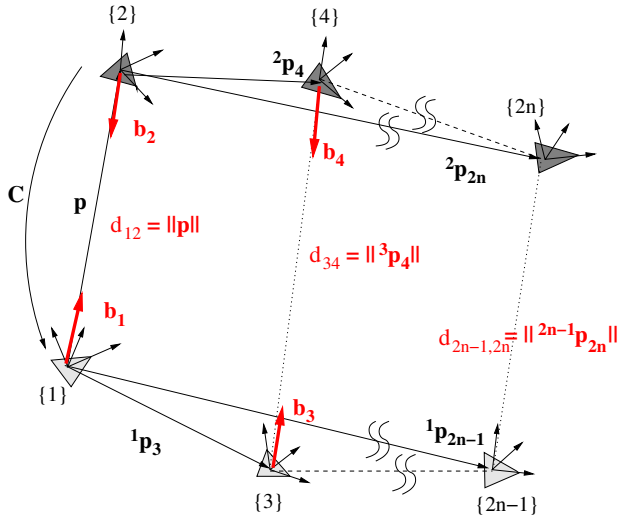

Fig. 1. Geometry of the robot trajectories. The odd (even) numbered frames of reference depict the consecutive poses of robot R_1 (R_2). The distance between the robot poses $\{i\}$ and $\{j\}$ is denoted by d_{ij}, $i \in \{1, 3, \ldots, 2n-1\}$, $j \in \{2, 4, \ldots, 2n\}$. $\mathbf{b}_i$ ($\mathbf{b}_j$) is a unit vector pointing from $\{i\}$ to $\{j\}$ ($\{j\}$ to $\{i\}$) expressed in the initial frame $\{1\}$ ($\{2\}$). The objective is to determine the transformation between the robots' initial frames $\{1\}$ and $\{2\}$, parameterized by the translation vector $\mathbf{p}$ and the rotation matrix $\mathbf{C}$.

In contrast to the case of motion in 2D, very little is known about motion-induced extrinsic calibration in 3D. Specifically, previous research has focused on the problem of determining relative pose using range-only measurements, which corresponds to System 14 in our analysis.[3] Interestingly, in the minimal problem setting, the task of relative-pose estimation using only distance measurements is equivalent to the forward-kinematics problem of the general Stewart-Gough platform [23], which has 40 (generally complex) solutions [20]: these can be found by solving a system of multivariate polynomial equations [21], [22]. Moreover, in our recent work [24], we presented methods for determining the robots' relative poses for the special case of *overdetermined homogeneous* robot pairs (i.e., the *same* type of observations to both robots at every time step and the total number of measurements is *larger* than the number of unknown DOF). However, to the best of our knowledge, no algorithms exist for determining 3D relative pose using different *combinations* of robot-to-robot distance and/or bearing measurements over time, e.g., the robots can measure distance at the first time step, bearing at the second time step, etc. This paper intends to fill this gap, and also addresses the most challenging case where only the minimum number of necessary measurements is available. We start our discussion in the next section with the problem formulation and the introduction of the 14 base minimal systems.

III. Problem Formulation

The following notation is used in this paper:

[3]Since this base minimal problem has been sufficiently addressed in the existing literature, we omit its detailed description and refer the interested reader to [20]–[22] for an in-depth analysis of the solution methodology.

- ${}^i\mathbf{p}_j$ Position of frame $\{j\}$ expressed in frame $\{i\}$. i and j are used for denoting robot poses. Odd numbers correspond to robot R_1 and even numbers correspond to robot R_2.
- ${}^i_j\mathbf{C}$ Rotation matrix that projects vectors expressed in frame $\{j\}$ to frame $\{i\}$.
- $\mathbf{C}(\mathbf{u}, \alpha)$ Rotation matrix describing a rotation about the unit vector $\mathbf{u}$ by an angle α.
- $\lfloor \mathbf{u} \times \rfloor$ Skew-symmetric matrix of $\mathbf{u}$ so that $\lfloor \mathbf{u} \times \rfloor \mathbf{v} = \mathbf{u} \times \mathbf{v}$.
- d_{ij} Distance between the origins of frames $\{i\}$ and $\{j\}$.
- $\mathbf{b}_i$ The bearing from robot R_1 to R_2 when R_1 is at pose $\{i\} = \{2n-1\}, n \in \mathbb{N}^*$, expressed in frame $\{1\}$.
- $\mathbf{b}_j$ The bearing from robot R_2 to R_1 when R_2 is at pose $\{j\} = \{2n\}, n \in \mathbb{N}^*$, expressed in frame $\{2\}$.
- $s\alpha$ Short for $\sin(\alpha)$.
- $c\alpha$ Short for $\cos(\alpha)$.

Consider two robots R_1 and R_2 moving randomly[4] in 3D through a sequence of poses $\{1\}, \{3\}, \ldots, \{2n-1\}$ for R_1, and $\{2\}, \{4\}, \ldots, \{2n\}$ for R_2 (see Fig. 1). Along their trajectories, the robots estimate their positions, ${}^1\mathbf{p}_i$ and ${}^2\mathbf{p}_j$, $i \in \{1, 3, ..., 2n-1\}$, $j \in \{2, 4, ..., 2n\}$, with respect to their initial frames, as well as their orientations, represented by the rotation matrices ${}^1_i\mathbf{C}$ and ${}^2_j\mathbf{C}$, respectively (e.g., by integrating linear and rotational velocity measurements over time). Additionally, at time-step t_n when robots R_1 and R_2 reach poses $\{i = 2n-1\}$ and $\{j = 2n\}$, respectively, each robot can measure the range and/or bearing towards the other robot. The range between the robots is given by $d_{ij} = ||{}^i\mathbf{p}_j||$, and the bearing is described by a unit vector expressed in the current local frame, ${}^i\mathbf{b}_j$ for robot R_1 and ${}^j\mathbf{b}_i$ for robot R_2. Later on, we will also need these unit vectors expressed in the robots' initial frames and, thus, we define $\mathbf{b}_i := {}^1_i\mathbf{C}\,{}^i\mathbf{b}_j$ and $\mathbf{b}_j := {}^2_j\mathbf{C}\,{}^j\mathbf{b}_i$. At each time step, the two robots can measure a *subset* of these measurements: $\{d_{ij}, \mathbf{b}_i, \mathbf{b}_j\}$.

Our goal is to use the ego-motion estimates and the relative pose measurements to determine the 6-DOF initial transformation between the two robots, i.e., their relative position $\mathbf{p} := {}^1\mathbf{p}_2$ and orientation $\mathbf{C} := {}^1_2\mathbf{C}$. In this paper, we only focus on solving the minimal problems where the number of measurement constraints equals the number of unknowns. In what follows, we will show that only the 14 systems listed in Fig. 2 need to be considered, while all other combinations of inter-robot measurements result into problems equivalent to these 14 systems.

IV. The 14 Base Minimal Problems

We start by noting that there are 7 possible combinations of inter-robot measurements at each time step: $\{d_{ij}, \mathbf{b}_i, \mathbf{b}_j\}$, $\{\mathbf{b}_i, \mathbf{b}_j\}$, $\{d_{ij}, \mathbf{b}_i\}$, $\{d_{ij}, \mathbf{b}_j\}$, $\{\mathbf{b}_i\}$, $\{\mathbf{b}_j\}$, $\{d_{ij}\}$, and at most 6 time steps need to be considered if, e.g., only a distance measurement is recorded at each time step. Since each distance measurement provides one constraint on the relative pose, we need 6 distance measurements to determine the 6-DOF relative pose. Evidently, when the measurements provide more constraints, we need less than 6 time steps. This naive analysis will give us 7^6 cases. Fortunately, we can reduce this number significantly by considering only the minimal problems and using problem equivalence based on the following lemma.

[4]As it will become evident later on, the coefficients of the polynomials describing the geometric relation between the robots' poses depend on their trajectories and one can use this fact to enforce simplifications by appropriately restricting the robots' motions. In this work, however, we are interested in the most general and challenging case, where the robots are allowed to follow arbitrary trajectories.

	t_1	t_2	t_3	t_4	t_5	t_6	r
1	$d_{12}, \mathbf{b}_1, \mathbf{b}_2$	d_{34}					2
2	$\mathbf{b}_1, \mathbf{b}_2$	$\mathbf{b}_3$					2
3	$d_{12}, \mathbf{b}_1$	$d_{34}, \mathbf{b}_3$					∞
4	$d_{12}, \mathbf{b}_1$	$d_{34}, \mathbf{b}_4$					∞
5	$\mathbf{b}_1, \mathbf{b}_2$	d_{34}	d_{56}				4
6	$d_{12}, \mathbf{b}_1$	$\mathbf{b}_3$	d_{56}				4
7	$d_{12}, \mathbf{b}_1$	$\mathbf{b}_4$	d_{56}				4
8	$\mathbf{b}_1$	$\mathbf{b}_3$	$\mathbf{b}_5$				8
9	$\mathbf{b}_1$	$\mathbf{b}_3$	$\mathbf{b}_6$				8
10	$d_{12}, \mathbf{b}_1$	d_{34}	d_{56}	d_{78}			8
11	$\mathbf{b}_1$	$\mathbf{b}_3$	d_{56}	d_{78}			16
12	$\mathbf{b}_1$	$\mathbf{b}_4$	d_{56}	d_{78}			16
13	$\mathbf{b}_1$	d_{34}	d_{56}	d_{78}	$d_{9,10}$		28
14	d_{12}	d_{34}	d_{56}	d_{78}	$d_{9,10}$	$d_{11,12}$	40

Fig. 2. The 14 base minimal problems. Under column t_i are measurements recorded at time step i. The last column (under r) shows the number of solutions to each system. System 14 is not covered in this paper, because it is addressed in [20]–[22].

Lemma 1: One instance of the relative pose problem can be transformed to an equivalent problem by the following two operations:

1) Changing the order of the robots.
2) Changing the order of the measurements taken.

Proof: In order to establish problem equivalence, we here demonstrate how to use the solution of the transformed problem (i.e., when the order of the robots or measurements has changed) to solve the original problem (i.e., determine ${}^1_2\mathbf{C}$ and ${}^1\mathbf{p}_2$).

First, if we exchange the order of the robots, i.e., rename robot R_2 as R_1 and vice versa, the solution of the transformed problem is $({}^2_1\mathbf{C},\ {}^2\mathbf{p}_1)$. Therefore, the solution of the original system is computed from the inverse transformation: ${}^1_2\mathbf{C} = {}^2_1\mathbf{C}^T$, ${}^1\mathbf{p}_2 = -{}^1_2\mathbf{C}^2\mathbf{p}_1$.

Exchanging the order of inter-robot measurements will only make a difference to the problem formulation when the swapping involves measurements recorded at the first time step, since the unknown variables are the 6-DOF initial robot-to-robot transformation. Without loss of generality, assume that measurements taken at the first and second time steps are swapped. Then the solution of the transformed system is actually the transformation $({}^3_4\mathbf{C},\ {}^3\mathbf{p}_4)$ between the frames of reference $\{3\}$ and $\{4\}$ of the original system. The solution of the original system can then be computed using: ${}^1_2\mathbf{C} = {}^1_3\mathbf{C}\,{}^3_4\mathbf{C}\,{}^2_4\mathbf{C}^T$, and ${}^1\mathbf{p}_2 = {}^1\mathbf{p}_3 + {}^1_3\mathbf{C}^3\mathbf{p}_4 - {}^1_2\mathbf{C}^2\mathbf{p}_4$. ■

Now we will describe the process for identifying the 14 minimal systems. First of all, since we are only interested in minimal systems, where the number of equations equals the number of unknowns, we only need to consider combinations of measurements that provide exactly 6 equations. A distance

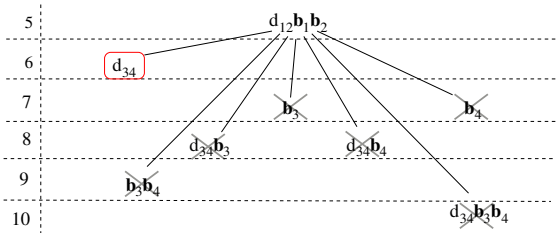

(a) Expansions providing more than 6 constraints are removed.

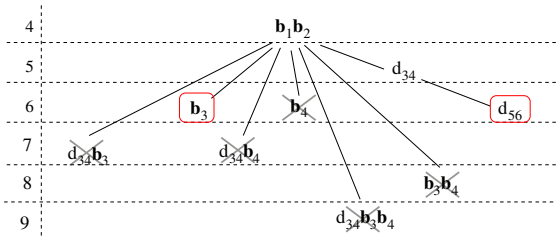

(b) Expansion $\mathbf{b}_4$ is removed since it is equivalent to $\mathbf{b}_3$ by exchanging the order of robots.

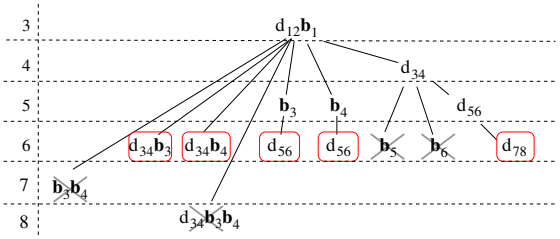

(c) The two combinations $\{d_{12}, \mathbf{b}_1; d_{34}; \mathbf{b}_5\}$ and $\{d_{12}, \mathbf{b}_1; d_{34}; \mathbf{b}_6\}$ are removed since they are equivalent to $\{d_{12}, \mathbf{b}_1; \mathbf{b}_3; d_{56}\}$ and $\{d_{12}, \mathbf{b}_1; \mathbf{b}_4; d_{56}\}$ by changing the order of measurements.

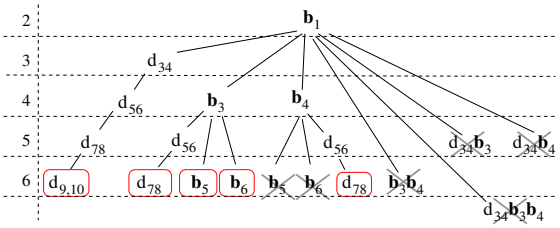

(d) $\{\mathbf{b}_1; \mathbf{b}_4; \mathbf{b}_5\}$ and $\{\mathbf{b}_1; \mathbf{b}_4; \mathbf{b}_6\}$ are equivalent to $\{\mathbf{b}_1; \mathbf{b}_3; \mathbf{b}_6\}$ by changing the order of measurements, or by changing the order of robots and order of measurements. Other nodes: $\{d_{34}, \mathbf{b}_3, \mathbf{b}_4\}$, $\{\mathbf{b}_3, \mathbf{b}_4\}$, $\{d_{34}, \mathbf{b}_3\}$ and $\{d_{34}, \mathbf{b}_4\}$, are removed since they are considered in (a), (b), and (c) as root nodes.

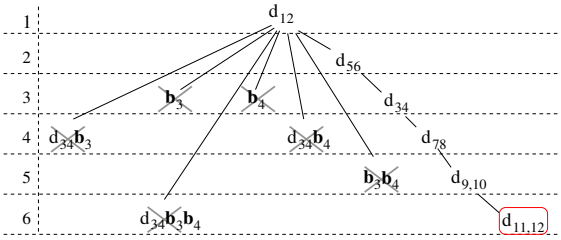

(e) The only case we need to consider is the distance-only case. All other cases have been considered in previous expansions.

Fig. 3. Measurement expansion trees. The numbers on the left of each graph denote the number of constraints provided by the measurements. Since we are only interested in minimal systems, all nodes having more than 6 constraints are removed. The leaf nodes marked by "X" are the ones removed. The nodes marked with red boxes are the 14 base systems. Note that inside { }, the measurements recorded at the same (consecutive) time step are separated by a comma (semicolon).

measurement provides one equation, and a bearing measurement provides two. So we will collect measurements until we accumulate 6 constraints. To keep track of these combinations, we use an expansion tree (see Fig. 3) and prune its branches using Lemma 1.

At the first time step, we can exclude $\{\mathbf{b}_2\}$ and $\{d_{12}, \mathbf{b}_2\}$ from the 7 combinations by changing the order of the robots. Hence, we only need to expand 5 sets of measurements: $\{d_{12}, \mathbf{b}_1, \mathbf{b}_2\}$, $\{\mathbf{b}_1, \mathbf{b}_2\}$, $\{d_{12}, \mathbf{b}_1\}$, $\{\mathbf{b}_1\}$, $\{d_{12}\}$. We will discuss each one of them in the following:

(a) Starting from $\{d_{12}, \mathbf{b}_1, \mathbf{b}_2\}$ we only need to include $\{d_{34}\}$, since all other choices are overdetermined systems [see Fig. 3(a)].

(b) From $\{\mathbf{b}_1, \mathbf{b}_2\}$ we need to consider two cases: $\{\mathbf{b}_3\}$, and $\{d_{34}\}$. Besides removing overdetermined systems, we can also remove $\{\mathbf{b}_4\}$ by exchanging the order of the robots [see Fig. 3(b)]. Moreover, we only need to keep $\{d_{56}\}$ from the possible expansions of $\{d_{34}\}$, since all other problems are overdetermined.

(c) From $\{d_{12}, \mathbf{b}_1\}$ we can exclude two second level expansions from $\{d_{34}\}$ [see Fig. 3(c)], since $\{d_{12}, \mathbf{b}_1; d_{34}; \mathbf{b}_5\}$ and $\{d_{12}, \mathbf{b}_1; d_{34}; \mathbf{b}_6\}$ are equivalent to $\{d_{12}, \mathbf{b}_1; \mathbf{b}_3; d_{56}\}$ and $\{d_{12}, \mathbf{b}_1; \mathbf{b}_4; d_{56}\}$, respectively, by changing the order of the measurements.

(d) Similarly, from $\{\mathbf{b}_1\}$ we can exclude two second level expansions from $\{\mathbf{b}_4\}$, since $\{\mathbf{b}_1; \mathbf{b}_4; \mathbf{b}_5\}$ is equivalent to $\{\mathbf{b}_1; \mathbf{b}_3; \mathbf{b}_6\}$ by changing the order of measurements, and $\{\mathbf{b}_1; \mathbf{b}_4; \mathbf{b}_6\}$ is also equivalent to $\{\mathbf{b}_1; \mathbf{b}_3; \mathbf{b}_6\}$ by first exchanging the order of the robots and then changing the order of measurements. The other cases $\{d_{34}, \mathbf{b}_3, \mathbf{b}_4\}$, $\{\mathbf{b}_3, \mathbf{b}_4\}$, and $\{d_{34}, \mathbf{b}_3\}$ have already been considered in the first three expansions (a)–(c) as root nodes. $\{d_{34}, \mathbf{b}_4\}$ is also considered in (c) after changing the order of the robots.

(e) Finally, for branches expanding from $\{d_{12}\}$, we only need to consider the distance-only case [see Fig. 3(e)], since all other cases have also been considered before.

Adding all the cases together, we have a total of 14 base minimal systems listed in Fig. 2. A summary of the problem formulation and solutions of these minimal systems are listed in Table III. Next, we will present closed-form or analytical solutions to these problems.

V. Algebraic Solutions to the Minimal Problems of Systems 1 and 2

For System 1, we measure $\{d_{12}, \mathbf{b}_1, \mathbf{b}_2; d_{34}\}$, and for System 2, we measure $\{\mathbf{b}_1, \mathbf{b}_2; \mathbf{b}_3\}$. Since the mutual bearing measurements $\mathbf{b}_1$ and $\mathbf{b}_2$ appear in both systems, their equations have similar structure and can be solved using the same approach. In this section, we will first derive the systems of equations for both problems, and then provide their solutions.

A. System 1: Measurements $\{d_{12}, \mathbf{b}_1, \mathbf{b}_2; d_{34}\}$

For this problem, the relative position is directly measured as $\mathbf{p} = d_{12}\mathbf{b}_1$. Therefore, we only need to compute the relative orientation, parameterized by $\mathbf{C}$.

From the mutual bearing measurements $\mathbf{b}_1$ and $\mathbf{b}_2$, we have the following constraint:

$$\mathbf{b}_1 + \mathbf{C}\mathbf{b}_2 = \mathbf{0} \tag{1}$$

Additionally, by expanding the constraint from the distance measurement d_{34}, we have

$$\begin{aligned} &{}^3\mathbf{p}_4^T {}^3\mathbf{p}_4 \\ &= (\mathbf{p} + \mathbf{C}^2\mathbf{p}_4 - {}^1\mathbf{p}_3)^T {}^1_3\mathbf{C}^1_3\mathbf{C}^T(\mathbf{p} + \mathbf{C}^2\mathbf{p}_4 - {}^1\mathbf{p}_3) \\ &= (\mathbf{p} + \mathbf{C}^2\mathbf{p}_4 - {}^1\mathbf{p}_3)^T(\mathbf{p} + \mathbf{C}^2\mathbf{p}_4 - {}^1\mathbf{p}_3) = d_{34}^2 \\ \Rightarrow &\mathbf{v}^T\mathbf{C}^2\mathbf{p}_4 + a = 0 \end{aligned} \tag{2}$$

where $\mathbf{v} = 2(\mathbf{p} - {}^1\mathbf{p}_3)$ and $a = \mathbf{p}^T\mathbf{p} + {}^2\mathbf{p}_4^T {}^2\mathbf{p}_4 + {}^1\mathbf{p}_3^T {}^1\mathbf{p}_3 - 2\mathbf{p}^T {}^1\mathbf{p}_3 - d_{34}^2$ are known quantities.

The last step of the solution process is to find $\mathbf{C}$ from equations (1) and (2), which is described in Section V-C.

B. System 2: Measurements $\{\mathbf{b}_1, \mathbf{b}_2; \mathbf{b}_3\}$

For this system, besides the mutual bearing constraint (1), we have the following equation using $\mathbf{b}_1$ and $\mathbf{b}_3$, which is the sum of vectors from $\{1\}$, through $\{2\}$, $\{4\}$, $\{3\}$ and back to $\{1\}$ (see Fig. 1):

$$\begin{aligned} &\mathbf{p} + \mathbf{C}^2\mathbf{p}_4 - {}^1_3\mathbf{C}^3\mathbf{p}_4 - {}^1\mathbf{p}_3 = \mathbf{0} \\ \Rightarrow\ &d_{12}\mathbf{b}_1 + \mathbf{C}^2\mathbf{p}_4 - d_{34}\mathbf{b}_3 - {}^1\mathbf{p}_3 = \mathbf{0}. \end{aligned} \tag{3}$$

If the rotation $\mathbf{C}$ is known, the relative position can be found by first determining the distance d_{12}. To do this, we eliminate d_{34} from equation (3) by forming the cross product with $\mathbf{b}_3$, i.e.,

$$d_{12}\lfloor \mathbf{b}_3 \times \rfloor \mathbf{b}_1 + \lfloor \mathbf{b}_3 \times \rfloor \mathbf{C}^2\mathbf{p}_4 - \lfloor \mathbf{b}_3 \times \rfloor {}^1\mathbf{p}_3 = \mathbf{0} \tag{4}$$

where $\lfloor \mathbf{b}_3 \times \rfloor$ is a 3×3 skew-symmetric matrix corresponding to the cross product. Then d_{12} can be computed from (4) by forming the dot product with $\lfloor \mathbf{b}_3 \times \rfloor \mathbf{b}_1$, i.e.,

$$d_{12} = \frac{(\lfloor \mathbf{b}_3 \times \rfloor \mathbf{b}_1)^T \lfloor \mathbf{b}_3 \times \rfloor ({}^1\mathbf{p}_3 - \mathbf{C}^2\mathbf{p}_4)}{(\lfloor \mathbf{b}_3 \times \rfloor \mathbf{b}_1)^T (\lfloor \mathbf{b}_3 \times \rfloor \mathbf{b}_1)} \tag{5}$$

The relative position is then readily available as $\mathbf{p} = d_{12}\mathbf{b}_1$. Next, we will describe how to compute $\mathbf{C}$.

The unknown distances d_{12} and d_{34} can be eliminated from equation (3) by projecting it on $\mathbf{v} = \mathbf{b}_1 \times \mathbf{b}_3$, i.e., the cross product of $\mathbf{b}_1$ and $\mathbf{b}_3$:

$$\mathbf{v}^T\mathbf{C}^2\mathbf{p}_4 - \mathbf{v}^T {}^1\mathbf{p}_3 = 0 \tag{6}$$

If we define a scalar $a := -\mathbf{v}^T {}^1\mathbf{p}_3$, then it is easy to see that equations (6) and (2) have identical structure.

C. Rotation Matrix Determination

We have shown that for both Systems 1 and 2, in order to determine the rotation matrix $\mathbf{C}$, we need to solve the following system of equations:

$$\mathbf{b}_1 + \mathbf{C}\mathbf{b}_2 = \mathbf{0} \tag{7}$$

$$\mathbf{v}^T\mathbf{C}^2\mathbf{p}_4 + a = 0 \tag{8}$$

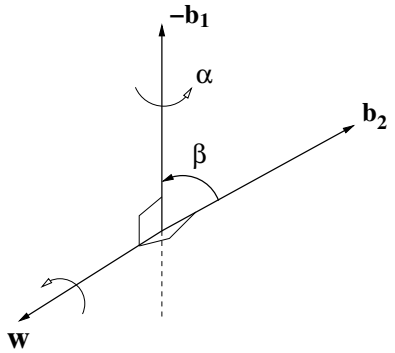

Fig. 4. A rotation that satisfies the constraint $\mathbf{b}_1 + \mathbf{C}\mathbf{b}_2 = \mathbf{0}$, where $\mathbf{w} = \frac{\mathbf{b}_1 \times \mathbf{b}_2}{||\mathbf{b}_1 \times \mathbf{b}_2||}$.

The key idea behind our approach is to first exploit the geometric properties of (7) which will allow us to determine two degrees of freedom in rotation. The remaining unknown degree of freedom can subsequently be computed using (8).

We start by first showing the following lemma (see Fig. 4).

Lemma 2: A particular solution to (7) is $\mathbf{C}^* = \mathbf{C}(\mathbf{w}, \beta)$, where $\mathbf{w} = \frac{\mathbf{b}_1 \times \mathbf{b}_2}{||\mathbf{b}_1 \times \mathbf{b}_2||}$, and $\beta = Atan2(||\mathbf{b}_1 \times \mathbf{b}_2||, -\mathbf{b}_1^T\mathbf{b}_2)$.

Proof: Using the Rodrigues rotation formula, we have

$$\mathbf{C}(\mathbf{w}, \beta) = c\beta\mathbf{I} + s\beta\lfloor \mathbf{w} \times \rfloor + (1 - c\beta)\mathbf{w}\mathbf{w}^T \tag{9}$$

where $\lfloor \mathbf{w} \times \rfloor$ is the skew-symmetric matrix of $\mathbf{w}$, so that $\lfloor \mathbf{w} \times \rfloor \mathbf{b}_2 = \mathbf{w} \times \mathbf{b}_2$. Substituting $\mathbf{C}(\mathbf{w}, \beta)$ in (7), we have

$$-\mathbf{b}_1 = (c\beta\mathbf{I} + s\beta\lfloor \mathbf{w} \times \rfloor + (1 - c\beta)\mathbf{w}\mathbf{w}^T)\mathbf{b}_2 \tag{10}$$

$$\Rightarrow -\mathbf{b}_1 = c\beta\mathbf{b}_2 + s\beta\lfloor \mathbf{w} \times \rfloor \mathbf{b}_2 \tag{11}$$

Projecting (11) on $\mathbf{b}_2$, yields:

$$c\beta = -\mathbf{b}_1^T\mathbf{b}_2. \tag{12}$$

Premultiplying both sides of (11) with $\lfloor \mathbf{b}_2 \times \rfloor$ yields,

$$\begin{aligned} -\lfloor \mathbf{b}_2 \times \rfloor \mathbf{b}_1 &= s\beta\lfloor \mathbf{b}_2 \times \rfloor \lfloor \mathbf{w} \times \rfloor \mathbf{b}_2 \\ \Rightarrow \mathbf{w}||\mathbf{b}_1 \times \mathbf{b}_2|| &= -s\beta\lfloor \mathbf{b}_2 \times \rfloor \lfloor \mathbf{b}_2 \times \rfloor \mathbf{w} \\ \Rightarrow \mathbf{w}||\mathbf{b}_1 \times \mathbf{b}_2|| &= -s\beta(-\mathbf{I} + \mathbf{b}_2\mathbf{b}_2^T)\mathbf{w} \\ \Rightarrow \mathbf{w}||\mathbf{b}_1 \times \mathbf{b}_2|| &= s\beta\mathbf{w} \\ \Rightarrow s\beta &= ||\mathbf{b}_1 \times \mathbf{b}_2|| \end{aligned} \tag{13}$$

■

We next show the general form of solutions of (7) in Lemma 3.

Lemma 3: Any solution of (7) assumes the form $\mathbf{C} = \mathbf{C}(\mathbf{w}, \beta)\mathbf{C}(\mathbf{b}_2, \alpha) = \mathbf{C}(-\mathbf{b}_1, \alpha)\mathbf{C}(\mathbf{w}, \beta)$, where α is an unknown angle to be determined.

Proof: Given that $\mathbf{C}(\mathbf{w}, \beta)$ is a particular solution of (7), i.e.,

$$-\mathbf{b}_1 = \mathbf{C}(\mathbf{w}, \beta)\mathbf{b}_2 \tag{14}$$

we seek to find all matrices $\mathbf{C}$ that satisfy (7). From (7) and (14), we have

$$\begin{aligned} \mathbf{C}\mathbf{b}_2 = -\mathbf{b}_1 &= \mathbf{C}(\mathbf{w}, \beta)\mathbf{b}_2 \\ \Rightarrow \mathbf{C}(\mathbf{w}, -\beta)\mathbf{C}\mathbf{b}_2 &= \mathbf{b}_2 \end{aligned} \tag{15}$$

Since $\mathbf{b}_2 = \mathbf{C}(\mathbf{b}_2, \alpha)\mathbf{b}_2$ for any α, we have

$$\begin{aligned} &\mathbf{C}(\mathbf{w}, -\beta)\mathbf{C} = \mathbf{C}(\mathbf{b}_2, \alpha) \\ \Rightarrow\ &\mathbf{C} = \mathbf{C}(\mathbf{w}, \beta)\mathbf{C}(\mathbf{b}_2, \alpha). \end{aligned} \tag{16}$$

We now prove the second part of the lemma, i.e., that $\mathbf{C} = \mathbf{C}(-\mathbf{b}_1, \alpha)\mathbf{C}(\mathbf{w}, \beta)$. Substituting the Rodrigues formula in (16) to expand $\mathbf{C}(\mathbf{b}_2, \alpha)$, we have

$$\mathbf{C} = \mathbf{C}(\mathbf{w}, \beta)(c\alpha\mathbf{I} + s\alpha\lfloor \mathbf{b}_2 \times \rfloor + (1 - c\alpha)\mathbf{b}_2\mathbf{b}_2^T) \tag{17}$$

$$= c\alpha\mathbf{C}(\mathbf{w}, \beta) + s\alpha\mathbf{C}(\mathbf{w}, \beta)\lfloor \mathbf{b}_2 \times \rfloor + (1 - c\alpha)\mathbf{C}(\mathbf{w}, \beta)\mathbf{b}_2\mathbf{b}_2^T \tag{18}$$

$$= c\alpha\mathbf{C}(\mathbf{w}, \beta) + s\alpha\lfloor \mathbf{C}(\mathbf{w}, \beta)\mathbf{b}_2 \times \rfloor\mathbf{C}(\mathbf{w}, \beta) + (1 - c\alpha)(\mathbf{C}(\mathbf{w}, \beta)\mathbf{b}_2)(\mathbf{C}(\mathbf{w}, \beta)\mathbf{b}_2)^T\mathbf{C}(\mathbf{w}, \beta) \tag{19}$$

$$= [c\alpha\mathbf{I} + s\alpha\lfloor \mathbf{C}(\mathbf{w}, \beta)\mathbf{b}_2 \times \rfloor + (1 - c\alpha) \cdot (\mathbf{C}(\mathbf{w}, \beta)\mathbf{b}_2)(\mathbf{C}(\mathbf{w}, \beta)\mathbf{b}_2)^T]\mathbf{C}(\mathbf{w}, \beta) \tag{20}$$

$$= \mathbf{C}(\mathbf{C}(\mathbf{w}, \beta)\mathbf{b}_2, \alpha)\mathbf{C}(\mathbf{w}, \beta) \tag{21}$$

$$= \mathbf{C}(-\mathbf{b}_1, \alpha)\mathbf{C}(\mathbf{w}, \beta) \tag{22}$$

where for the last equality, we used (14), while from (18) to (19) we employed the equality $\mathbf{C}(\mathbf{w}, \beta)\lfloor \mathbf{b}_2 \times \rfloor = \lfloor \mathbf{C}(\mathbf{w}, \beta)\mathbf{b}_2 \times \rfloor \mathbf{C}(\mathbf{w}, \beta)$.

■

The last step of this process is to substitute $\mathbf{C} = \mathbf{C}(-\mathbf{b}_1, \alpha)\mathbf{C}(\mathbf{w}, \beta)$ into (8) to determine α, i.e.,

$$0 = \mathbf{v}^T\mathbf{C}(-\mathbf{b}_1, \alpha)^2\mathbf{p}_4' + a \tag{23}$$

where ${}^2\mathbf{p}_4' = \mathbf{C}(\mathbf{w}, \beta)^2\mathbf{p}_4$.

Substituting the Rodrigues formula for $\mathbf{C}(-\mathbf{b}_1, \alpha)$ in (23), yields,

$$\begin{aligned} &\mathbf{v}^T(c\alpha\mathbf{I} + s\alpha\lfloor -\mathbf{b}_1 \times \rfloor + (1 - c\alpha)\mathbf{b}_1\mathbf{b}_1^T)^2\mathbf{p}_4' + a \\ =&\underbrace{(\mathbf{v}^T{}^2\mathbf{p}_4' - \mathbf{v}^T\mathbf{b}_1\mathbf{b}_1^T{}^2\mathbf{p}_4')}_{l_1}c\alpha - \underbrace{(\mathbf{v}^T\lfloor \mathbf{b}_1 \times \rfloor{}^2\mathbf{p}_4')}_{l_2}s\alpha \\ &+ \underbrace{\mathbf{v}^T\mathbf{b}_1\mathbf{b}_1^T{}^2\mathbf{p}_4' + a}_{l_3} = 0 \\ \Rightarrow &c\alpha = \frac{l_2 s\alpha - l_3}{l_1} \end{aligned} \tag{24, 25}$$

Finally, substituting (25) into the trigonometric constraint $c\alpha^2 + s\alpha^2 = 1$, we arrive at a quadratic polynomial in $s\alpha$.

$$m_0 s\alpha^2 + m_1 s\alpha + m_2 = 0$$

where $m_0 = l_1^2 + l_2^2$, $m_1 = -2l_2l_3$, and $m_2 = l_3^2 - l_1^2$. Back substituting the two solutions for $s\alpha$ into equation (25), we get two solutions for $c\alpha$.

$$s\alpha_1 = \frac{-m_1 + \triangle}{2m_0}, \qquad s\alpha_2 = \frac{-m_1 - \triangle}{2m_0} \tag{26}$$

$$c\alpha_1 = \frac{-l_2(m_1 - \triangle)}{2l_1m_0} - \frac{l_3}{l_1}, \quad c\alpha_2 = \frac{-l_2(m_1 + \triangle)}{2l_1m_0} - \frac{l_3}{l_1} \tag{27}$$

where $\triangle = \sqrt{m_1^2 - 4m_0m_2}$.

Therefore, there exist up to two distinct[5] solutions for the transformation between frames $\{1\}$ and $\{2\}$. When additional robot-to-robot measurements are available, we can use them to disambiguate which one corresponds to the true relative transformation, because only one of the two solutions will also satisfy those extra measurements constraints.

[5]In case $\triangle = 0$, these two solutions collapse to one.

VI. Unidentifiability of Systems 3 and 4

For these two systems, we will show that there exist infinite solutions for the rotation $\mathbf{C}$. In this situation, we need to wait for additional inter-robot measurements and solve for the relative pose using one of the other minimal problems.

A. System 3: Measurements $\{d_{12}, \mathbf{b}_1; d_{34}, \mathbf{b}_3\}$

Let us first examine System 3. Substituting the measurements d_{12}, $\mathbf{b}_1$, d_{34}, and $\mathbf{b}_3$ in equation (3), we have only one geometric constraint for $\mathbf{C}$

$$\begin{aligned} &\mathbf{p} + \mathbf{C}^2\mathbf{p}_4 - {}_3^1\mathbf{C}^3\mathbf{p}_4 - {}^1\mathbf{p}_3 = 0 \\ \Rightarrow\ &d_{12}\mathbf{b}_1 + \mathbf{C}^2\mathbf{p}_4 - d_{34}\mathbf{b}_3 - {}^1\mathbf{p}_3 = 0 \\ \Rightarrow\ &(d_{12}\mathbf{b}_1 - d_{34}\mathbf{b}_3 - {}^1\mathbf{p}_3) + \mathbf{C}^2\mathbf{p}_4 = 0 \end{aligned} \tag{28}$$

where, as evident, the rotation around the unit vector in the direction of $d_{12}\mathbf{b}_1 - d_{34}\mathbf{b}_3 - {}^1\mathbf{p}_3$ is undetermined.

B. System 4: Measurements $\{d_{12}, \mathbf{b}_1; d_{34}, \mathbf{b}_4\}$

Similarly, System 4 also has one degree of freedom in rotation undetermined. The difference is that the vector ${}^4\mathbf{p}_3$ is measured instead of vector ${}^3\mathbf{p}_4$.

$$\mathbf{p} + \mathbf{C}^2\mathbf{p}_4 + \mathbf{C}\,{}_4^2\mathbf{C}^4\mathbf{p}_3 - {}^1\mathbf{p}_3 = 0 \tag{29}$$

$$\Rightarrow \mathbf{p} - {}^1\mathbf{p}_3 + \mathbf{C}({}^2\mathbf{p}_4 + d_{34}\mathbf{b}_4) = 0 \tag{30}$$

In this case, the rotation around $\mathbf{p} - {}^1\mathbf{p}_3$ is undetermined. Therefore, these two systems have infinite number of solutions.

VII. Algebraic Solutions to the Minimal Problem of System 5

For System 5, the available measurements are $\{\mathbf{b}_1, \mathbf{b}_2; d_{34}; d_{56}\}$. Using the mutual bearing measurements $\mathbf{b}_1$ and $\mathbf{b}_2$, we can again express the rotation matrix as $\mathbf{C} = \mathbf{C}(-\mathbf{b}_1, \alpha)\mathbf{C}(\mathbf{w}, \beta)$ (see Lemma 3), where $\mathbf{b}_1$, $\mathbf{w}$, and β are known while α as well as d_{12} can be computed from the two distance constraints:

$$(d_{12}\mathbf{b}_1 + \mathbf{C}^2\mathbf{p}_4 - {}^1\mathbf{p}_3)^T(d_{12}\mathbf{b}_1 + \mathbf{C}^2\mathbf{p}_4 - {}^1\mathbf{p}_3) = d_{34}^2 \tag{31}$$

$$(d_{12}\mathbf{b}_1 + \mathbf{C}^2\mathbf{p}_6 - {}^1\mathbf{p}_5)^T(d_{12}\mathbf{b}_1 + \mathbf{C}^2\mathbf{p}_6 - {}^1\mathbf{p}_5) = d_{56}^2 \tag{32}$$

After expanding the above two equations, we have

$$d_{12}^2 + 2d_{12}(\mathbf{b}_1^T\mathbf{C}^2\mathbf{p}_4 - \mathbf{b}_1^T{}^1\mathbf{p}_3) - 2{}^1\mathbf{p}_3^T\mathbf{C}^2\mathbf{p}_4 + \epsilon_1 = 0 \tag{33}$$

$$d_{12}^2 + 2d_{12}(\mathbf{b}_1^T\mathbf{C}^2\mathbf{p}_6 - \mathbf{b}_1^T{}^1\mathbf{p}_5) - 2{}^1\mathbf{p}_5^T\mathbf{C}^2\mathbf{p}_6 + \epsilon_2 = 0 \tag{34}$$

where $\epsilon_1 = {}^2\mathbf{p}_4^T{}^2\mathbf{p}_4 + {}^1\mathbf{p}_3^T{}^1\mathbf{p}_3 - d_{34}^2$, and $\epsilon_2 = {}^2\mathbf{p}_6^T{}^2\mathbf{p}_6 + {}^1\mathbf{p}_5^T{}^1\mathbf{p}_5 - d_{56}^2$ are known. Substituting $\mathbf{C} = \mathbf{C}(-\mathbf{b}_1, \alpha)\mathbf{C}(\mathbf{w}, \beta)$ in (33) and (34) yields,

$$d_{12}^2 + 2d_{12}\mathbf{b}_1^T({}^2\mathbf{p}_4' - {}^1\mathbf{p}_3) - 2{}^1\mathbf{p}_3^T\mathbf{C}(-\mathbf{b}_1, \alpha)^2\mathbf{p}_4' + \epsilon_1 = 0 \tag{35}$$

$$d_{12}^2 + 2d_{12}\mathbf{b}_1^T({}^2\mathbf{p}_6' - {}^1\mathbf{p}_5) - 2{}^1\mathbf{p}_5^T\mathbf{C}(-\mathbf{b}_1, \alpha)^2\mathbf{p}_6' + \epsilon_2 = 0 \tag{36}$$

where we have used the property $\mathbf{b}_1^T\mathbf{C}(-\mathbf{b}_1,\alpha)=\mathbf{b}_1^T$ and set ${}^2\mathbf{p}'_4=\mathbf{C}(\mathbf{w},\beta)^2\mathbf{p}_4$, ${}^2\mathbf{p}'_6=\mathbf{C}(\mathbf{w},\beta)^2\mathbf{p}_6$. Employing the Rodrigues formula for $\mathbf{C}(-\mathbf{b}_1,\alpha)$ in (35)–(36) yields:

$$\mathbf{L}\begin{bmatrix}c\alpha\\ s\alpha\end{bmatrix}=\boldsymbol{\xi}\Rightarrow\begin{bmatrix}c\alpha\\ s\alpha\end{bmatrix}=\mathbf{L}^{-1}\boldsymbol{\xi} \tag{37}$$

where

$$\mathbf{L}=2\begin{bmatrix}{}^1\mathbf{p}_3^T(\mathbf{I}-\mathbf{b}_1\mathbf{b}_1^T)^2\mathbf{p}'_4 & -{}^1\mathbf{p}_3^T\lfloor\mathbf{b}_1\times\rfloor^2\mathbf{p}'_4\\ {}^1\mathbf{p}_5^T(\mathbf{I}-\mathbf{b}_1\mathbf{b}_1^T)^2\mathbf{p}'_6 & -{}^1\mathbf{p}_5^T\lfloor\mathbf{b}_1\times\rfloor^2\mathbf{p}'_6\end{bmatrix} \tag{38}$$

is a known 2×2 matrix, while each of the two components of $\boldsymbol{\xi}$ is quadratic in the unknown d_{12}, i.e.,

$$\boldsymbol{\xi}=\begin{bmatrix}d_{12}^2+2d_{12}\mathbf{b}_1^T({}^2\mathbf{p}'_4-{}^1\mathbf{p}_3)-2({}^1\mathbf{p}_3^T\mathbf{b}_1)({}^2\mathbf{p}_4'^T\mathbf{b}_1)+\epsilon_1\\ d_{12}^2+2d_{12}\mathbf{b}_1^T({}^2\mathbf{p}'_6-{}^1\mathbf{p}_5)-2({}^1\mathbf{p}_5^T\mathbf{b}_1)({}^2\mathbf{p}_6'^T\mathbf{b}_1)+\epsilon_2\end{bmatrix}.$$

Taking the norm of both sides of (37) and employing the trigonometric constraint $c\alpha^2+s\alpha^2=1$, gives

$$\boldsymbol{\xi}^T\mathbf{L}^{-T}\mathbf{L}^{-1}\boldsymbol{\xi}=1 \tag{39}$$

which is a 4^{th} order univariate polynomial in d_{12} which can be solved in closed form [25] to yield up to four real solutions for d_{12}. Back-substituting each positive root of (39) in (37) provides a unique solution for the rotation angle α, and hence the rotation matrix $\mathbf{C}$. Therefore, there exist up to four solutions for the relative robot-to-robot transformation of System 5.

VIII. Algebraic Solutions to the Minimal Problems of Systems 6 and 7

Due to their similarities, Systems 6 and 7 can be formulated as an identically structured system of equations and solved using the same methodology. Note that in both systems, the relative position $\mathbf{p}=d_{12}\mathbf{b}_1$ is directly measured and the unknown quantities are in the rotation matrix $\mathbf{C}$. In the following sections, we first derive the system of equations for both problems, and then present the closed-form solution.

A. System 6: Measurements $\{d_{12},\ \mathbf{b}_1;\ \mathbf{b}_3;\ d_{56}\ \}$

Given the relative position $\mathbf{p}=d_{12}\mathbf{b}_1$ and the second bearing measurement $\mathbf{b}_3$, we have the following constraint, which is the sum of vectors from $\{1\}$ through $\{2\}$, $\{4\}$, $\{3\}$, and back to $\{1\}$ (see Fig. 1):

$$\begin{aligned}\mathbf{p}+\mathbf{C}^2\mathbf{p}_4-\tfrac{1}{3}\mathbf{C}^3\mathbf{p}_4-{}^1\mathbf{p}_3&=0\\ \Rightarrow\mathbf{p}+\mathbf{C}^2\mathbf{p}_4-d_{34}\mathbf{b}_3-{}^1\mathbf{p}_3&=0. &(40)\\ \Rightarrow\lfloor\mathbf{b}_3\times\rfloor({}^1\mathbf{p}_3-\mathbf{p})&=\lfloor\mathbf{b}_3\times\rfloor\mathbf{C}^2\mathbf{p}_4 &(41)\end{aligned}$$

where we have multiplied both sides of (40) with the cross-product matrix $\lfloor\mathbf{b}_3\times\rfloor$ to eliminate d_{34}.

Finally, by expanding the constraint from the distance measurement d_{56}, we have the third equation necessary for solving the 3-DOF relative orientation $\mathbf{C}$.

$$\begin{aligned}{}^5\mathbf{p}_6^T{}^5\mathbf{p}_6=(\mathbf{p}+\mathbf{C}^2\mathbf{p}_6-{}^1\mathbf{p}_5)^T(\mathbf{p}+\mathbf{C}^2\mathbf{p}_6-{}^1\mathbf{p}_5)&=d_{56}^2\\ \Rightarrow 2(\mathbf{p}-{}^1\mathbf{p}_5)^T\mathbf{C}^2\mathbf{p}_6+\epsilon&=0 &(42)\end{aligned}$$

where $\epsilon=\mathbf{p}^T\mathbf{p}+{}^2\mathbf{p}_6^T{}^2\mathbf{p}_6+{}^1\mathbf{p}_5^T{}^1\mathbf{p}_5-2\mathbf{p}^T{}^1\mathbf{p}_5-d_{56}^2$.

B. System 7: Measurements $\{d_{12},\ \mathbf{b}_1;\ \mathbf{b}_4;\ d_{56}\}$

Similar to System 6, we have the following constraint from the first three measurements.

$$\begin{aligned}\mathbf{p}+\mathbf{C}^2\mathbf{p}_4+\mathbf{C}_4^2\mathbf{C}^4\mathbf{p}_3-{}^1\mathbf{p}_3&=0 &(43)\\ \Rightarrow\mathbf{C}^T(\mathbf{p}-{}^1\mathbf{p}_3)+{}^2\mathbf{p}_4+d_{34}\mathbf{b}_4&=0 &(44)\\ \Rightarrow\lfloor\mathbf{b}_4\times\rfloor^2\mathbf{p}_4=\lfloor\mathbf{b}_4\times\rfloor\mathbf{C}^T({}^1\mathbf{p}_3-\mathbf{p})&&(45)\end{aligned}$$

where we have multiplied both sides of (44) with the cross-product matrix $\lfloor\mathbf{b}_4\times\rfloor$ to eliminate d_{34}. Together with the distance constraint (42), rewritten as

$$2{}^2\mathbf{p}_6^T\mathbf{C}^T(\mathbf{p}-{}^1\mathbf{p}_5)+\epsilon=0 \tag{46}$$

we have three equations for solving $\mathbf{C}^T$.

C. Closed-form Solution for the Rotation Matrix

For System 6, we need to determine the rotation matrix $\mathbf{C}$ (or $\mathbf{C}^T$ for System 7) from equations of the form [see (41), (42) and (45), (46)]:

$$\begin{aligned}\lfloor\mathbf{b}\times\rfloor\mathbf{u}&=\lfloor\mathbf{b}\times\rfloor\mathbf{C}\mathbf{v} &(47)\\ \mathbf{u}'^T\mathbf{C}\mathbf{v}'+a&=0 &(48)\end{aligned}$$

where $\mathbf{u}$, $\mathbf{v}$, $\mathbf{u}'$, $\mathbf{v}'$ and a are known, and $\mathbf{b}$ is a unit vector. In our solution method, we will exploit the results of Section V-C [see (7), (8)]. To do so, we first show the following:

Lemma 4: The rotational matrices satisfying (47), also satisfy the following equations:

$$\begin{aligned}\mathbf{C}\mathbf{v}&=\gamma_1\mathbf{b}+\mathbf{u} &(49)\\ \text{or}\quad\mathbf{C}\mathbf{v}&=\gamma_2\mathbf{b}+\mathbf{u} &(50)\end{aligned}$$

where $\gamma_1=-\mathbf{b}^T\mathbf{u}+\sqrt{(\mathbf{b}^T\mathbf{u})^2+||\mathbf{v}||^2-||\mathbf{u}||^2}$ and $\gamma_2=-\mathbf{b}^T\mathbf{u}-\sqrt{(\mathbf{b}^T\mathbf{u})^2+||\mathbf{v}||^2-||\mathbf{u}||^2}$.

Proof: We start by rewriting (47) as

$$\lfloor\mathbf{b}\times\rfloor(\mathbf{C}\mathbf{v}-\mathbf{u})=0. \tag{51}$$

Hence, the vector $\mathbf{b}$ must satisfy

$$\gamma\mathbf{b}=(\mathbf{C}\mathbf{v}-\mathbf{u}) \tag{52}$$

where γ is a scalar whose value is to be determined.

We rewrite (52) as:

$$\mathbf{C}\mathbf{v}=\gamma\mathbf{b}+\mathbf{u} \tag{53}$$

Computing the norm square of both sides of (53), we obtain a quadratic polynomial in γ:

$$\begin{aligned}||\mathbf{v}||^2&=(\gamma\mathbf{b}+\mathbf{u})^T(\gamma\mathbf{b}+\mathbf{u}) &(54)\\ &=\gamma^2\mathbf{b}^T\mathbf{b}+\mathbf{u}^T\mathbf{u}+2\gamma\mathbf{b}^T\mathbf{u} &(55)\\ \Rightarrow\gamma^2+2\gamma\mathbf{b}^T\mathbf{u}+||\mathbf{u}||^2-||\mathbf{v}||^2&=0 &(56)\end{aligned}$$

where we have employed $\mathbf{b}^T\mathbf{b}=1$. There are two solutions for γ

$$\begin{aligned}\gamma_1&=-\mathbf{b}^T\mathbf{u}+\sqrt{(\mathbf{b}^T\mathbf{u})^2+||\mathbf{v}||^2-||\mathbf{u}||^2} &(57)\\ \gamma_2&=-\mathbf{b}^T\mathbf{u}-\sqrt{(\mathbf{b}^T\mathbf{u})^2+||\mathbf{v}||^2-||\mathbf{u}||^2}. &(58)\end{aligned}$$

Substituting γ_1 and γ_2 in (53) and dividing both sides with γ_1 or γ_2 yields (49) and (50).

■

Combining each of the (49)-(50) with (48) provides the following two systems of equations

$$\left.\begin{array}{c}\mathbf{C}\mathbf{v}=\gamma_1\mathbf{b}+\mathbf{u}\\ \mathbf{u}'^T\mathbf{C}\mathbf{v}'+a=0\end{array}\right\}\Sigma_1 \text{ or } \left.\begin{array}{c}\mathbf{C}\mathbf{v}=\gamma_2\mathbf{b}+\mathbf{u}\\ \mathbf{u}'^T\mathbf{C}\mathbf{v}'+a=0\end{array}\right\}\Sigma_2 \quad (59)$$

Note that both (Σ_1) and (Σ_2) have identical structures as (7)–(8). Thus, by employing the approach of Section V-C, we can compute up to two solutions for each of them, for a total of up to four solutions for Systems 6 and 7.

IX. Analytical Solutions to the Minimal Problems of Systems 8, 9, and 10

In the following, we first derive the system of equations for these three problems, and then present our analytic solutions. In our approach, we first solve for the rotation matrix $\mathbf{C}$ and then compute the translation vector $\mathbf{p}$.

A. System 8: Measurements $\{\mathbf{b}_1;\ \mathbf{b}_3;\ \mathbf{b}_5\ \}$

From Fig. 1, using pairwise the measurements $\mathbf{b}_1$ and $\mathbf{b}_3$, and $\mathbf{b}_1$ and $\mathbf{b}_5$, we have the following two constraints

$$d_{12}\mathbf{b}_1+\mathbf{C}^2\mathbf{p}_4-d_{34}\mathbf{b}_3-{}^1\mathbf{p}_3=0 \quad (60)$$
$$d_{12}\mathbf{b}_1+\mathbf{C}^2\mathbf{p}_6-d_{56}\mathbf{b}_5-{}^1\mathbf{p}_5=0 \quad (61)$$

whose difference gives:

$$d_{34}\mathbf{b}_3+\mathbf{C}({}^2\mathbf{p}_6-{}^2\mathbf{p}_4)-d_{56}\mathbf{b}_5-({}^1\mathbf{p}_5-{}^1\mathbf{p}_3)=0. \quad (62)$$

If the rotation matrix $\mathbf{C}$ was known, we can solve for d_{12} by first eliminating the unknown d_{34} from (60) by forming the cross product with $\mathbf{b}_3$ [see (5)]. Then, the relative translation is $\mathbf{p}=d_{12}\mathbf{b}_1$.

Next, we describe how to eliminate all the unknown distances, d_{12}, d_{34}, and d_{56}, from (60), (61), and (62), so that we can solve for $\mathbf{C}$. Specifically, we define three vectors

$$\mathbf{v}_1=\mathbf{b}_1\times\mathbf{b}_3,\quad \mathbf{v}_2=\mathbf{b}_1\times\mathbf{b}_5,\quad \mathbf{v}_3=\mathbf{b}_3\times\mathbf{b}_5 \quad (63)$$

and form their dot products with (60), (61), and (62), respectively:

$$\mathbf{v}_1^T\mathbf{C}^2\mathbf{p}_4-\mathbf{v}_1^T{}^1\mathbf{p}_3=0 \quad (64)$$
$$\mathbf{v}_2^T\mathbf{C}^2\mathbf{p}_6-\mathbf{v}_2^T{}^1\mathbf{p}_5=0 \quad (65)$$
$$\mathbf{v}_3^T\mathbf{C}({}^2\mathbf{p}_6-{}^2\mathbf{p}_4)-\mathbf{v}_3^T({}^1\mathbf{p}_5-{}^1\mathbf{p}_3)=0. \quad (66)$$

From these three equations, we determine $\mathbf{C}$ (see Section IX-D).

B. System 9: Measurements $\{\mathbf{b}_1;\ \mathbf{b}_3;\ \mathbf{b}_6\ \}$

Systems 9 and 8 both contain measurements $\mathbf{b}_1$ and $\mathbf{b}_3$. Therefore, System 9 also contains equation (64). The differences lie in the next two constraints using $\mathbf{b}_1$ and $\mathbf{b}_6$, and $\mathbf{b}_3$ and $\mathbf{b}_6$:

$$d_{12}\mathbf{b}_1+\mathbf{C}^2\mathbf{p}_6+d_{56}\mathbf{C}\mathbf{b}_6-{}^1\mathbf{p}_5=0 \quad (67)$$
$$d_{34}\mathbf{b}_3+\mathbf{C}({}^2\mathbf{p}_6-{}^2\mathbf{p}_4)+d_{56}\mathbf{C}\mathbf{b}_6-({}^1\mathbf{p}_5-{}^1\mathbf{p}_3)=0. \quad (68)$$

Similarly to System 8, we define

$$\mathbf{v}_1=\mathbf{b}_1\times\mathbf{b}_3,\quad \mathbf{v}_2=\mathbf{b}_1\times\mathbf{C}\mathbf{b}_6,\quad \mathbf{v}_3=\mathbf{b}_3\times\mathbf{C}\mathbf{b}_6 \quad (69)$$

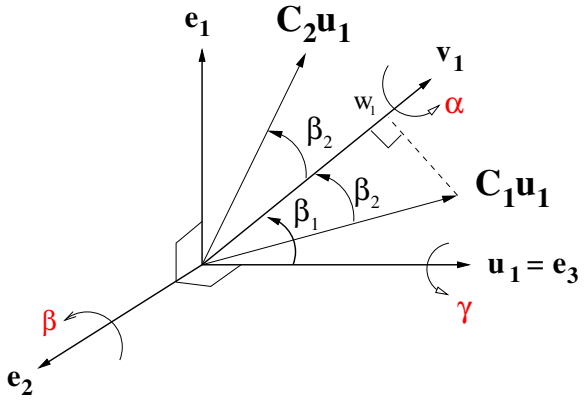

Fig. 5. Sequence of rotations that satisfies the constraint: $\mathbf{v}_1^T\mathbf{C}\mathbf{u}_1=w_1$. Let $\mathbf{e}_3=\mathbf{u}_1$, $\mathbf{e}_2=\frac{\mathbf{u}_1\times\mathbf{v}_1}{||\mathbf{u}_1\times\mathbf{v}_1||}$ (if $\mathbf{u}_1\parallel\mathbf{v}_1$, $\mathbf{e}_2$ is any unit vector perpendicular to $\mathbf{u}_1$), and $\mathbf{e}_1=\mathbf{e}_2\times\mathbf{e}_3$. Rotating around $\mathbf{e}_2$ by $\beta=\beta_1-\beta_2$ or $\beta=\beta_1+\beta_2$ satisfies $\mathbf{v}_1^T\mathbf{C}\mathbf{u}_1=w_1$. The constraint is satisfied for arbitrary rotations around the other two axes $\mathbf{u}_1$ and $\mathbf{v}_1$.

and project equation (67) to $\mathbf{v}_2$ to obtain

$$(\mathbf{b}_1\times\mathbf{C}\mathbf{b}_6)^T\mathbf{C}^2\mathbf{p}_6-{}^1\mathbf{p}_5^T(\mathbf{b}_1\times\mathbf{C}\mathbf{b}_6)=0 \quad (70)$$
$$\Rightarrow \mathbf{b}_1^T(\mathbf{C}\mathbf{b}_6\times\mathbf{C}^2\mathbf{p}_6)-({}^1\mathbf{p}_5\times\mathbf{b}_1)^T\mathbf{C}\mathbf{b}_6=0 \quad (71)$$
$$\Rightarrow \mathbf{b}_1^T\mathbf{C}(\mathbf{b}_6\times{}^2\mathbf{p}_6)-({}^1\mathbf{p}_5\times\mathbf{b}_1)^T\mathbf{C}\mathbf{b}_6=0 \quad (72)$$

where from (70) to (71), we have applied the identity $(\mathbf{a}\times\mathbf{b})^T\mathbf{c}=\mathbf{a}^T(\mathbf{b}\times\mathbf{c})$.

Similarly, projecting (68) to $\mathbf{v}_3$, yields

$$\mathbf{b}_3^T\mathbf{C}\mathbf{u}_3-\mathbf{u}_2^T\mathbf{C}\mathbf{b}_6=0 \quad (73)$$

where $\mathbf{u}_3=\mathbf{b}_6\times({}^2\mathbf{p}_6-{}^2\mathbf{p}_4)$, and $\mathbf{u}_2=({}^1\mathbf{p}_5-{}^1\mathbf{p}_3)\times\mathbf{b}_3$. Finally, from (64), (72), and (73), we solve for $\mathbf{C}$ (see Section IX-D). Note also that, once $\mathbf{C}$ is determined, d_{12} is computed from (60) after forming the cross product with $\mathbf{b}_3$ [see (5)].

C. System 10: Measurements $\{d_{12},\ \mathbf{b}_1;\ d_{34};\ d_{56};\ d_{78}\ \}$

In this problem, the relative position is known from $\mathbf{p}=d_{12}\mathbf{b}_1$. The remaining quantity to be determined is the rotation matrix $\mathbf{C}$. From the three distance measurements $d_{2i-1,2i}$, $i=2,\ 3,\ 4$, we have [see (42)]:

$$2(\mathbf{p}-{}^1\mathbf{p}_{2i-1})^T\mathbf{C}^2\mathbf{p}_{2i}+\epsilon_i=0,\ i=2,\ 3,\ 4 \quad (74)$$

where $\epsilon_i=\mathbf{p}^T\mathbf{p}+{}^2\mathbf{p}_{2i}^T{}^2\mathbf{p}_{2i}+{}^1\mathbf{p}_{2i-1}^T{}^1\mathbf{p}_{2i-1}-2\mathbf{p}^T{}^1\mathbf{p}_{2i-1}-d_{2i-1,2i}^2$.

D. Analytical Solution for the Rotation Matrix

Systems 8, 9, and 10 share the same form of equations for solving $\mathbf{C}$, i.e.,

$$f_1=\mathbf{v}_1^T\mathbf{C}\mathbf{u}_1-w_1=0 \quad (75)$$
$$f_i=\sum\mathbf{v}_i^T\mathbf{C}\mathbf{u}_i-w_i=0,\quad i=2,\ 3. \quad (76)$$

where we have normalized (75) to make the vectors $\mathbf{v}_1$ and $\mathbf{u}_1$ unit vectors.

Instead of using rotations around perpendicular axes, in this case we parameterize the rotation matrix as a product of three consecutive rotations around axes spanning 3-DOF:

$$\mathbf{C} = \mathbf{C}(\mathbf{v}_1, \alpha)\mathbf{C}(\mathbf{e}_2, \beta)\mathbf{C}(\mathbf{u}_1, \gamma) \tag{77}$$

where $\mathbf{e}_2 := \frac{\mathbf{u}_1 \times \mathbf{v}_1}{||\mathbf{u}_1 \times \mathbf{v}_1||}$ if $\mathbf{v}_1$ is not parallel to $\mathbf{u}_1$, otherwise $\mathbf{e}_2$ is any unit vector perpendicular to $\mathbf{u}_1$. Substituting (77) in (75), we have

$$\mathbf{v}_1^T \mathbf{C}(\mathbf{e}_2, \beta)\mathbf{u}_1 - w_1 = 0 \tag{78}$$

From the geometry[6] of Fig. 5, we can find two particular solutions for the rotational angle β

$$\beta = \beta_1 - \beta_2 = \arccos(\mathbf{u}_1^T \mathbf{v}_1) - \arccos(w_1), \text{ or} \tag{79}$$

$$\beta = \beta_1 + \beta_2 = \arccos(\mathbf{u}_1^T \mathbf{v}_1) + \arccos(w_1). \tag{80}$$

However, later on we will prove that choosing any one of the two solutions leads to exactly the same set of 8 solutions for the relative rotation matrix. For now, we select the first solution for β and continue solving for the other two rotation angles.

Next, we will find the rotation angles α and γ from the next two equations.

$$\sum \mathbf{v}_2^T \mathbf{C}(\mathbf{v}_1, \alpha)\mathbf{C}(\mathbf{e}_2, \beta)\mathbf{C}(\mathbf{u}_1, \gamma)\mathbf{u}_2 = w_2 \tag{81}$$

$$\sum \mathbf{v}_3^T \mathbf{C}(\mathbf{v}_1, \alpha)\mathbf{C}(\mathbf{e}_2, \beta)\mathbf{C}(\mathbf{u}_1, \gamma)\mathbf{u}_3 = w_3 \tag{82}$$

Since β is known, the above equations are bilinear in $c\alpha$, $s\alpha$ and $c\gamma$, $s\gamma$. Substituting the Rodrigues formula

$$\mathbf{C}(\mathbf{u}_1, \gamma) = c\gamma\mathbf{I} + s\gamma\lfloor \mathbf{u}_1 \times \rfloor + (1 - c\gamma)\mathbf{u}_1\mathbf{u}_1^T \tag{83}$$

in (81), we have

$$\begin{aligned}
&\sum \mathbf{v}_2^T \mathbf{C}(\mathbf{v}_1, \alpha)\mathbf{C}(\mathbf{e}_2, \beta)[(\mathbf{u}_2 - \mathbf{u}_1^T\mathbf{u}_2\mathbf{u}_1)c\gamma \\
&+ \lfloor \mathbf{u}_1 \times \rfloor \mathbf{u}_2 s\gamma + \mathbf{u}_1^T\mathbf{u}_2\mathbf{u}_1] = w_2 \\
\Rightarrow &\sum \mathbf{v}_2^T \mathbf{C}(\mathbf{v}_1, \alpha)\mathbf{C}(\mathbf{e}_2, \beta)(\mathbf{u}_2 - \mathbf{u}_1^T\mathbf{u}_2\mathbf{u}_1)c\gamma + \\
&\sum \mathbf{v}_2^T \mathbf{C}(\mathbf{v}_1, \alpha)\mathbf{C}(\mathbf{e}_2, \beta)\lfloor \mathbf{u}_1 \times \rfloor \mathbf{u}_2 s\gamma \\
= &w_2 - \sum \mathbf{v}_2^T \mathbf{C}(\mathbf{v}_1, \alpha)\mathbf{C}(\mathbf{e}_2, \beta)\mathbf{u}_1^T\mathbf{u}_2\mathbf{u}_1
\end{aligned} \tag{84}$$

Similarly, by substituting (83) in (82), we rewrite (81) and (82) as linear functions in $c\gamma$ and $s\gamma$.

$$\mathbf{A}\begin{bmatrix} c\gamma \\ s\gamma \end{bmatrix} = \begin{bmatrix} w_2 - \ell_1 \\ w_3 - \ell_2 \end{bmatrix} \tag{85}$$

$$\Rightarrow \begin{bmatrix} c\gamma \\ s\gamma \end{bmatrix} = \mathbf{A}^{-1}\begin{bmatrix} w_2 - \ell_1 \\ w_3 - \ell_2 \end{bmatrix} \tag{86}$$

where $\mathbf{A}$ and ℓ_1, ℓ_2 are linear in $c\alpha$ and $s\alpha$:

$$\begin{aligned}
\mathbf{A}_{1,1} &= \sum \mathbf{v}_2^T \mathbf{C}(\mathbf{v}_1, \alpha)\mathbf{C}(\mathbf{e}_2, \beta)(\mathbf{u}_2 - \mathbf{u}_1^T\mathbf{u}_2\mathbf{u}_1) \\
\mathbf{A}_{1,2} &= \sum \mathbf{v}_2^T \mathbf{C}(\mathbf{v}_1, \alpha)\mathbf{C}(\mathbf{e}_2, \beta)\lfloor \mathbf{u}_1 \times \rfloor \mathbf{u}_2 \\
\mathbf{A}_{2,1} &= \sum \mathbf{v}_3^T \mathbf{C}(\mathbf{v}_1, \alpha)\mathbf{C}(\mathbf{e}_2, \beta)(\mathbf{u}_3 - \mathbf{u}_1^T\mathbf{u}_3\mathbf{u}_1) \\
\mathbf{A}_{2,2} &= \sum \mathbf{v}_3^T \mathbf{C}(\mathbf{v}_1, \alpha)\mathbf{C}(\mathbf{e}_2, \beta)\lfloor \mathbf{u}_1 \times \rfloor \mathbf{u}_3 \\
\ell_1 &= \sum \mathbf{v}_2^T \mathbf{C}(\mathbf{v}_1, \alpha)\mathbf{C}(\mathbf{e}_2, \beta)\mathbf{u}_1^T\mathbf{u}_2\mathbf{u}_1 \\
\ell_2 &= \sum \mathbf{v}_3^T \mathbf{C}(\mathbf{v}_1, \alpha)\mathbf{C}(\mathbf{e}_2, \beta)\mathbf{u}_1^T\mathbf{u}_3\mathbf{u}_1.
\end{aligned}$$

[6]Alternatively, the two solutions can be found algebraically by substituting the Rodrigues formula for $\mathbf{C}(\mathbf{e}_2, \beta)$ in (78).

Note that $c\gamma$ and $s\gamma$ in (86) are rational functions whose numerator and denominator are quadratic functions in $c\alpha$ and $s\alpha$. Substituting them in the trigonometric constraint $c\gamma^2 + s\gamma^2 = 1$, and after some algebraic manipulation we obtain a 4^{th} order polynomial $f(c\alpha, s\alpha)$.

$$\begin{aligned}
f = &h_1 c\alpha^4 + (h_2 s\alpha + h_3)c\alpha^3 + (h_4 s\alpha^2 + h_5 s\alpha + h_6)c\alpha^2 \\
&+ (h_7 s\alpha^3 + h_8 s\alpha^2 + h_9 s\alpha + h_{10})c\alpha \\
&+ h_{11} s\alpha^4 + h_{12} s\alpha^3 + h_{13} s\alpha^2 + h_{14} s\alpha + h_{15}
\end{aligned} \tag{87}$$

where the coefficients h_l, $l = 1 \ldots 15$, are functions of the measured quantities $\mathbf{v}_i$, $\mathbf{u}_i$ and w_i, $i = 2, 3$.

Using the trigonometric constraint $c\alpha^2 + s\alpha^2 = 1$ and the Sylvester resultant [26], we eliminate the variable $s\alpha$ from (87), and arrive at an 8^{th} order univariate polynomial [27]:

$$g(s\alpha) = \sum_{i=0}^{8} k_i s\alpha^i. \tag{88}$$

which we solve analytically using the companion matrix [26]. Back-substituting each of the 8 solutions for $s\alpha$ in equation (87), we get one solution for $c\alpha$, because (87) is linear in $c\alpha$ after replacing all even order terms of $c\alpha^{2k}$ by $(1 - s\alpha^2)^k$ and $c\alpha^3$ by $(1 - s\alpha^2)c\alpha$. Finally, each pair of solutions for $c\alpha$ and $s\alpha$ corresponds to one solution for $c\gamma$ and $s\gamma$ using equation (86).

We now prove that the two particular solutions of β lead to the same set of 8 solutions for the rotation matrix. Let the two particular rotation matrices be $\mathbf{C}_1 = \mathbf{C}(\mathbf{e}_2, \beta_1 - \beta_2)$ and $\mathbf{C}_2 = \mathbf{C}(\mathbf{e}_2, \beta_1 + \beta_2)$. From the geometry of Fig. 5, we have:

$$\mathbf{C}_1\mathbf{u}_1 = \mathbf{C}(\mathbf{v}_1, 180^\circ)\mathbf{C}_2\mathbf{u}_1 \tag{89}$$

$$\Rightarrow \mathbf{C}_1^T\mathbf{C}(\mathbf{v}_1, 180^\circ)\mathbf{C}_2\mathbf{u}_1 = \mathbf{u}_1 \tag{90}$$

Therefore,

$$\mathbf{C}_1^T\mathbf{C}(\mathbf{v}_1, 180^\circ)\mathbf{C}_2 = \mathbf{C}(\mathbf{u}_1, \theta) \tag{91}$$

where θ as shown in the Appendix A, equals to 180°, i.e.,

$$\mathbf{C}_2 = \mathbf{C}(\mathbf{v}_1, -180^\circ)\mathbf{C}_1\mathbf{C}(\mathbf{u}_1, 180^\circ). \tag{92}$$

Given 8 solutions for the rotational matrix C corresponding to the particular solution $\mathbf{C}_1$:

$$\mathbf{C}_{1,i} = \mathbf{C}(\mathbf{v}_1, \alpha_i)\mathbf{C}_1\mathbf{C}(\mathbf{u}_1, \gamma_i), \quad i = 1 \ldots 8 \tag{93}$$

and another 8 solutions corresponding to the particular solution $\mathbf{C}_2$

$$\mathbf{C}_{2,j} = \mathbf{C}(\mathbf{v}_1, \alpha_j)\mathbf{C}_2\mathbf{C}(\mathbf{u}_1, \gamma_j), \quad j = 1 \ldots 8, \tag{94}$$

we assume that at least one of the $\mathbf{C}_{2,j}$'s is different from all the $\mathbf{C}_{1,i}$'s, i.e., there exists at least one j, e.g., $j = g$ such that $\mathbf{C}_{2,g} \neq \mathbf{C}_{1,i}$, $\forall i$. We will show that this will lead to a contradiction. Specifically, substituting (92) in (94) for $j = g$, we have:

$$\begin{aligned}
\mathbf{C}_{2,g} &= \mathbf{C}(\mathbf{v}_1, \alpha_g)\mathbf{C}(\mathbf{v}_1, -180^\circ)\mathbf{C}_1\mathbf{C}(\mathbf{u}_1, 180^\circ)\mathbf{C}(\mathbf{u}_1, \gamma_g) \\
&= \mathbf{C}(\mathbf{v}_1, \alpha_g - 180^\circ)\mathbf{C}_1\mathbf{C}(\mathbf{u}_1, \gamma_g + 180^\circ).
\end{aligned} \tag{95}$$

However, this would mean that we have a 9^{th} solution stemming from $\mathbf{C}_1$, which is impossible.

X. Analytical Solutions for Systems 11, 12, and 13

Up to now, we have derived closed-form or analytical (resulting in univariate polynomials) solutions for Systems 1–2 and 5–10. However, for Systems 11–13, it is very challenging to follow a similar process. Fortunately, recent progress in algebraic geometry has provided a symbolic-numerical method for constructing the multiplication matrix from whose eigenvectors, we can read off the solutions. In the following sections, we derive the polynomial equations for Systems 11, 12, and 13, and then present the symbolic-numerical method [28] we employed for solving these systems.

A. System 11: Measurements $\{\mathbf{b}_1;\ \mathbf{b}_3;\ d_{56};\ d_{78}\}$

For this problem, we first write the unknown d_{12} as a function of the rotation matrix $\mathbf{C}$. Then by substituting it into the geometric constraints for d_{56} and d_{78}, we form a system of polynomials only in the rotation parameters. Even though the total degree of the resulting system is higher than before eliminating d_{12}, it reduces the problem size and makes the computations faster, as we will see later on.

Specifically, from the geometric constraint involving the bearing measurements $\mathbf{b}_1$ and $\mathbf{b}_3$ [see (60)], we eliminate the unknown d_{34} by premultiplying both sides with $\lfloor \mathbf{b}_3 \times \rfloor$ and solve for d_{12} [see (5)]:

$$d_{12} = \mathbf{v}_1^T \mathbf{C}^2 \mathbf{p}_4 + a \tag{96}$$

where

$$\mathbf{v}_1 = -\frac{(\lfloor \mathbf{b}_3 \times \rfloor \mathbf{b}_1)^T \lfloor \mathbf{b}_3 \times \rfloor}{(\lfloor \mathbf{b}_3 \times \rfloor \mathbf{b}_1)^T (\lfloor \mathbf{b}_3 \times \rfloor \mathbf{b}_1)}, \quad a = -\mathbf{v}_1^{T\,1}\mathbf{p}_3. \tag{97}$$

We then substitute d_{12} [see (96)] into the following two distance constraints:

$$(\mathbf{p} + \mathbf{C}^2\mathbf{p}_6 - {}^1\mathbf{p}_5)^T(\mathbf{p} + \mathbf{C}^2\mathbf{p}_6 - {}^1\mathbf{p}_5) = d_{56}^2 \tag{98}$$
$$(\mathbf{p} + \mathbf{C}^2\mathbf{p}_8 - {}^1\mathbf{p}_7)^T(\mathbf{p} + \mathbf{C}^2\mathbf{p}_8 - {}^1\mathbf{p}_7) = d_{78}^2. \tag{99}$$

The resulting equations are functions of only $\mathbf{C}$

$$\begin{aligned}&(\mathbf{v}_1^T\mathbf{C}^2\mathbf{p}_4)^2 + 2(\mathbf{v}_1^T\mathbf{C}^2\mathbf{p}_4)(\mathbf{b}_1^T\mathbf{C}^2\mathbf{p}_6)\\ &+2\mathbf{b}_1^T\mathbf{u}_1(\mathbf{v}_1^T\mathbf{C}^2\mathbf{p}_4) + 2\mathbf{u}_1^T\mathbf{C}^2\mathbf{p}_6 + \epsilon_1 = 0\end{aligned} \tag{100}$$

$$\begin{aligned}&(\mathbf{v}_1^T\mathbf{C}^2\mathbf{p}_4)^2 + 2(\mathbf{v}_1^T\mathbf{C}^2\mathbf{p}_4)(\mathbf{b}_1^T\mathbf{C}^2\mathbf{p}_8)\\ &+2\mathbf{b}_1^T\mathbf{u}_2(\mathbf{v}_1^T\mathbf{C}^2\mathbf{p}_4) + 2\mathbf{u}_2^T\mathbf{C}^2\mathbf{p}_8 + \epsilon_2 = 0\end{aligned} \tag{101}$$

where

$$\begin{aligned}\mathbf{u}_1 &= a\mathbf{b}_1 - {}^1\mathbf{p}_5, \qquad \epsilon_1 = {}^2\mathbf{p}_6^{T\,2}\mathbf{p}_6 + \mathbf{u}_1^T\mathbf{u}_1 - d_{56}^2\\ \mathbf{u}_2 &= a\mathbf{b}_1 - {}^1\mathbf{p}_7, \qquad \epsilon_2 = {}^2\mathbf{p}_8^{T\,2}\mathbf{p}_8 + \mathbf{u}_2^T\mathbf{u}_2 - d_{78}^2.\end{aligned}$$

Finally, let $\mathbf{v}_2 = \mathbf{b}_1 \times \mathbf{b}_3$. Projecting (60) to $\mathbf{v}_2$ results in a third equation in $\mathbf{C}$

$$\mathbf{v}_2^T\mathbf{C}^2\mathbf{p}_4 - \mathbf{v}_2^{T\,1}\mathbf{p}_3 = 0. \tag{102}$$

Now, we have three equations (100)–(102) to solve for the 3-DOF rotation matrix $\mathbf{C}$.

We choose the (non-Hamiltonian) quaternion to parameterize orientation defined as $\bar{q} = [q_1\ q_2\ q_3\ q_4]^T = [\mathbf{q}^T\ q_4]^T$, and related to the rotational matrix as[7]

$$\mathbf{C}(\bar{q}) = \mathbf{I}_3 - 2q_4\lfloor \mathbf{q} \times \rfloor + 2\lfloor \mathbf{q} \times \rfloor^2. \tag{103}$$

Substituting (103) in (100) and (101) yields two 4^{th} order polynomials, while (102) is quadratic. Together with the unit-norm constraint

$$\bar{q}^T\bar{q} - 1 = 0 \tag{104}$$

forms a square system, which we can solve for $\bar{q}$. Once $\bar{q}$, and hence $\mathbf{C}$, is known (see Section X-D), we find d_{12} by back-substituting in (96).

B. System 12: Measurements $\{\mathbf{b}_1;\ \mathbf{b}_4;\ d_{56};\ d_{78}\}$

In this case, we cannot easily solve for d_{12} and $\mathbf{C}$ separately, because monomials containing both d_{12} and elements of $\mathbf{C}$ appear in the system. Instead, we form a square system of polynomial equations based on the available measurement constraints which we solve using the method described in Section X-D.

Specifically, multiplying (43) by $\mathbf{C}^T$ yields

$$d_{12}\mathbf{C}^T\mathbf{b}_1 + {}^2\mathbf{p}_4 + d_{34}\mathbf{b}_4 - \mathbf{C}^{T\,1}\mathbf{p}_3 = 0. \tag{105}$$

Then we eliminate d_{34} by forming the dot product with two unit vectors $\mathbf{v}_1$ and $\mathbf{v}_2$ both of which are perpendicular to $\mathbf{b}_4$, and obtain two equations:

$$d_{12}\mathbf{v}_i^T\mathbf{C}^T\mathbf{b}_1 - \mathbf{v}_i^T\mathbf{C}^{T\,1}\mathbf{p}_3 + \mathbf{v}_i^{T\,2}\mathbf{p}_4 = 0,\ i = 1,\ 2. \tag{106}$$

Expanding the distance constraints (98) and (99), we have

$$d_{12}^2 + 2d_{12}(\mathbf{b}_1^T\mathbf{C}^2\mathbf{p}_6 - \mathbf{b}_1^{T\,1}\mathbf{p}_5) - 2^1\mathbf{p}_5^T\mathbf{C}^2\mathbf{p}_6 + \epsilon_1 = 0 \tag{107}$$
$$d_{12}^2 + 2d_{12}(\mathbf{b}_1^T\mathbf{C}^2\mathbf{p}_8 - \mathbf{b}_1^{T\,1}\mathbf{p}_7) - 2^1\mathbf{p}_7^T\mathbf{C}^2\mathbf{p}_8 + \epsilon_2 = 0 \tag{108}$$

where

$$\epsilon_1 = {}^2\mathbf{p}_6^{T\,2}\mathbf{p}_6 + {}^1\mathbf{p}_5^{T\,1}\mathbf{p}_5 - d_{56}^2,\ \epsilon_2 = {}^2\mathbf{p}_8^{T\,2}\mathbf{p}_8 + {}^1\mathbf{p}_7^{T\,1}\mathbf{p}_7 - d_{78}^2.$$

Equations (106)–(108) and the unit-norm constraint (104) form a square system of five polynomial equations allowing us to solve for the relative pose.

C. System 13: Measurements $\{\mathbf{b}_1;\ d_{34};\ d_{56};\ d_{78};\ d_{9,10}\ \}$

From the bearing and distances measurements, we have the following constraints [see (107)], $i = 2, \ldots, 5$

$$d_{12}^2 + 2d_{12}(\mathbf{b}_1^T\mathbf{C}^2\mathbf{p}_{2i} - \mathbf{b}_1^{T\,1}\mathbf{p}_{2i-1}) - 2^1\mathbf{p}_{2i-1}^T\mathbf{C}^2\mathbf{p}_{2i} + \epsilon_i = 0$$

where $\epsilon_i = {}^2\mathbf{p}_{2i}^{T\,2}\mathbf{p}_{2i} + {}^1\mathbf{p}_{2i-1}^T{}^1\mathbf{p}_{2i-1} - d_{2i-1,2i}^2$. Together with the unit-norm constraint (104), we have a square system of five polynomial equations to solve for the relative pose.

[7] Note that since the quaternions $\bar{q}$ and $-\bar{q}$ both represent the same rotation, the number of solutions is double. One can easily eliminate the redundant solutions by discarding those with $q_4 < 0$.

D. Symbolic-Numeric Solution Method

In this section, we describe Reid and Zhi's symbolic-numeric method [28] for solving systems of multivariate polynomial equations and its application to our problems. This method computes the solutions via the multiplication matrix. We also refer the reader to [22] for a proof of Reid and Zhi's method, and to [29] for more details.

We expand each of the original systems of equations by multiplying them with monomials up to a certain total degree to form a new system

$$\mathbf{M}_t \mathbf{x}_t = \mathbf{0} \tag{109}$$

where $\mathbf{M}_t$ is a matrix containing all the coefficients of the expanded polynomial equations, and $\mathbf{x}_t$ is a vector of monomials up to total degree t. Therefore, the solutions of the system of polynomial equations must lie in the right null space of $\mathbf{M}_t$. The total degree is computed via a so-called involutive-form test. This test also tells us how many solutions the system has.

The involutive test includes prolongation and projection operations. A single prolongation of a system F means to expand it to one higher total degree. Prolongation up to total degree t is denoted by $F^{(t)}$. After each prolongation, we compute the null space of the coefficient matrix $\mathbf{M}_t$. A single projection means to remove rows of the vectors spanning the null space of $\mathbf{M}_t$ such that they contain monomials with one lower total degree, i.e., $\mathbf{x}_t$ reduces to $\mathbf{x}_{t-1}$. One projection of a system F is denoted by $\pi(F)$, and higher projection orders are denoted by $\pi^i(F)$, $i = 2, \ldots, t$.

A system F is involutive at order t and projection order ℓ if and only if $\pi^\ell(F^{(t)})$ satisfies [28]:

$$dim\ \pi^\ell(F^{(t)}) = dim\ \pi^{\ell+1}(F^{(t+1)}) = dim\ \pi^{\ell+1}(F^{(t)}) \tag{110}$$

where dim denotes the dimension of the corresponding space. Furthermore, $dim\ \pi^\ell(F^{(t)})$ equals the number of solutions of system F.

This involutive test only needs to be performed once offline. Once we know the total degree t to which to expand the system, we use it to construct $\mathbf{M}_t$ for all instances of the problem. Note that $\mathbf{M}_t$ is stored in symbolic form and is used to compute the multiplication matrix with respect to an unknown variable, in our case q_4[8]. The main steps to compute the multiplication matrix are listed in the following:

1) Compute the null space of $\mathbf{M}_t$, so that the columns of matrix $\mathbf{B}_t$ span its null space.
2) Perform ℓ and $\ell-1$ projections on $\mathbf{B}_t$, i.e., take the rows of $\mathbf{B}_t$ that correspond to monomials up to total degree $t-\ell$ and $t-\ell-1$ to form the new matrices $\mathbf{B}$ and $\mathbf{B}_1$, respectively.
3) Compute the SVD of $\mathbf{B}_1 = [\mathbf{U}_1\ \mathbf{U}_2] \cdot [\mathbf{S}\ \mathbf{0}]^T \cdot \mathbf{V}^T$.
4) Form the multiplication matrix of q_4 as $\mathbf{M}_{q_4} = \mathbf{U}_1^T \mathbf{B}_{q_4} \mathbf{V} \mathbf{S}^{-1}$, where $\mathbf{B}_{q_4}$ are the rows of $\mathbf{B}$ corresponding to monomials $q_4 \mathbf{x}_{t-\ell-1}$.
5) Compute the eigenvectors $\boldsymbol{\xi}_i$ of $\mathbf{M}_{q_4}$, and recover all solutions from the elements of $\mathbf{U}_1 \boldsymbol{\xi}_i$. The elements of this vector correspond to monomials in $\mathbf{x}_{t-\ell-1}$ evaluated at the solutions after proper scaling.

[8]In general, we can choose any variable as the multiplier as long as the solutions for this variable are distinct (see Ch. 2, Proposition 4.7 in [26]). In our specific problems at hand, we cannot choose d_{12}, because its solution multiplicity is at least two, since each solution for d_{12} corresponds to solutions $\bar{q}$ and $-\bar{q}$.

TABLE I
$dim\ \pi^\ell(F^{(t)})$ FOR SYSTEM 11

	t = 4	t = 5	t = 6	t = 7	t = 8	t = 9
$\ell = 0$	40	52	59	63	66	70
$\ell = 1$	25	39	45	47	48	50
$\ell = 2$	13	25	33	33	**32**	32
$\ell = 3$	5	13	25	33	**32**	**32**
$\ell = 4$	1	5	13	25	32	32
$\ell = 5$	0	1	5	13	25	32
$\ell = 6$	0	0	1	5	13	25
$\ell = 7$	0	0	0	1	5	13
$\ell = 8$	0	0	0	0	1	5
$\ell = 9$	0	0	0	0	0	1

For System 11, the involutive condition is met at total degree $t = 8$ and projection order $\ell = 2$. As shown in Table I, the number of solutions is 32. Since using quaternions introduces double solutions, the number of distinct solutions for the relative pose is 16. The size of the expanded coefficient matrix $\mathbf{M}_8$ is 560×495.

Both Systems 12 and 13 reach the involutive form at total degree $t = 8$, and they both have 5 variables, therefore the expanded coefficient matrices are both of size 1470×1287. However, System 12 reaches the involutive form at projection order $\ell = 3$ and has 16 solutions, while System 13 is involutive at $\ell = 1$ and has 28 solutions for the relative pose.

Since System 11 has a much smaller expanded coefficient matrix than System 12 and 13, its solution can be computed much faster. In our (unoptimized) Matlab implementation, solving System 11 takes 1.139 seconds, while solving System 12 and 13 takes 3.236 seconds and 4.397 seconds, respectively. Also note that our symbolic-numerical solvers are much faster than the iterative numerical solver, PHCpack [30]. It take PHC 2.983 seconds, 5.355 seconds, and 6.487 seconds to solve System 11, 12, and 13, respectively.

E. System 14: Measurements $\{d_{12};\ d_{34};\ d_{56};\ d_{78};\ d_{9,10};\ d_{11,12}\}$

From the six distance measurements, we have the following equations:

$$\mathbf{p}^T \mathbf{p} - d_{12}^2 = 0$$
$$(\mathbf{p} + \mathbf{C}^2 \mathbf{p}_{2i} - {}^1\mathbf{p}_{2i-1})^T (\mathbf{p} + \mathbf{C}^2 \mathbf{p}_{2i} - {}^1\mathbf{p}_{2i-1}) - d_{2i-1,2i}^2 = 0$$

where $i = 2, \ldots, 5$. This problem has been studied extensively in the literature; see [20]–[22] for its solution.

XI. SIMULATION RESULTS

We have evaluated the performance of our algorithms in simulation for different values of inter-robot measurement noise variance; however, omit tests with noise in the robots' ego-motion estimates, because the effect of perturbing the robots' ego-motion estimates is very similar to that of perturbing the inter-robot measurements.

The data for our simulations are generated as follows. First, we generate random robot trajectories in 3D, with the two robots starting at initial positions 1 m $\sim$ 2 m apart from each other, and moving 3 m $\sim$ 6 m between obtaining distance and/or bearing measurements. We perturb the true bearing direction to generate the bearing measurements. The perturbed bearing vectors are uniformly distributed in a cone with the true bearing as its main axis. The angle between the true vector and the boundary of the cone is defined as σ_b rad. The noise in the distance measurement[9] is assumed zero-mean white Gaussian with standard deviation $\sigma_d = 10\sigma_b$ m.

We conduct Monte Carlo simulations for different values of σ_b (the distance measurement noise standard deviation is $\sigma_d = 10\sigma_b$ for each value of σ_b), and report the averaged results of 1000 trials per setting for each system. We report the error in position as the 2-norm of the difference between the true and the estimated position[10]. To evaluate the error in the relative orientation, we use a multiplicative error model for the quaternion corresponding to the rotation matrix. In particular, true orientation, $\bar{q}$, estimated orientation, $\hat{\bar{q}}$, and error quaternion, $\delta\bar{q}$ are related via [31]:

$$\bar{q} = \delta\bar{q} \otimes \hat{\bar{q}} \tag{111}$$

where $\delta\bar{q}$ describes the small rotation that makes the estimated and the true orientation coincide. Using the small-angle approximation, the error quaternion can be written as

$$\delta\bar{q} \simeq \begin{bmatrix}\frac{1}{2}\delta\boldsymbol{\theta}^T & 1\end{bmatrix}^T \Leftrightarrow \mathbf{C} \simeq (\mathbf{I}_3 - \lfloor\delta\boldsymbol{\theta}\times\rfloor)\hat{\mathbf{C}} \tag{112}$$

and the 2-norm of $\delta\boldsymbol{\theta}$ is used to evaluate the orientation error.

Fig. 6 shows the orientation error and position error, respectively, as a function of the bearing noise σ_b for Systems 1, 2 and 5–13. The curves depict the median of the error in the 1000 trials, and the vertical bars show the 25 and 75 percentiles. As expected, the error increases as the standard deviation of the noise increases. We also see that the 75 percentiles are growing much faster than the 25 percentiles for most systems except for the position error of Systems 1, 6, 7, and 10. This indicates that the probability of having larger error in the relative pose estimate increases dramatically with the variance of the measurement noise. In contrast, the distribution of the position errors of Systems 1, 6, 7, and 10 remains almost the same, because it is directly measured from the distance d_{12} and bearing $\mathbf{b}_1$. Furthermore, systems with more bearing measurements achieve better accuracy than systems with more distance measurements. In particular, Systems 10 and 13 perform significantly worse than the other two systems in their group [see Figs. 6(e) and 6(g)]. Finally, we see that in the absence of measurement noise, we can recover the relative pose perfectly.

Lastly, we note that in all practical cases the solutions of the minimal problems should be used in conjunction with RANSAC [9] to perform outlier rejection followed by nonlinear least squares so as to improve the estimation accuracy using all available measurements.

[9]Without loss of generality, we assume that only one of the robots records range measurements at each location. If both robots measure the same distance, the two measurements can be combined first to provide a more accurate estimate of their distance.

[10]Since we focus on assessing the accuracy of the minimal problem solver, out of the multiple solutions, we choose as estimate the one closest to the true value. In practice, additional measurements are used to uniquely determine the position [19].

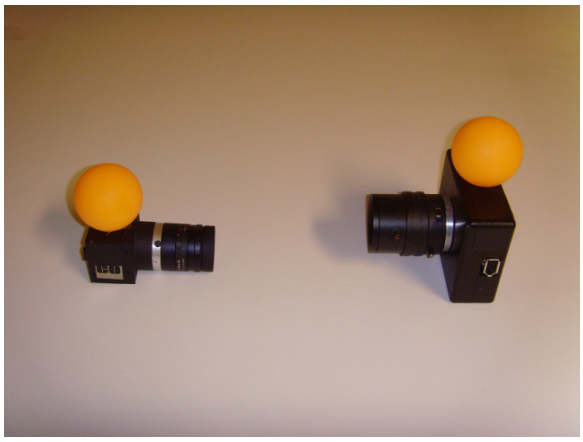

Fig. 7. The two cameras used in the experiment. The Point Grey Dragonfly camera is shown on the right, and the IDS uEye camera is on the left. The two ping-pong balls mounted on top of the two cameras are used as visual targets for measuring the distance and bearing between the two cameras.

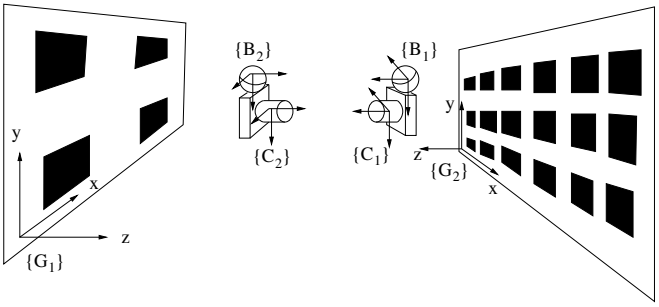

Fig. 8. The experimental setup. The Dragonfly camera, $\{C_1\}$, and the uEye camera, $\{C_2\}$, are looking at each other. The Dragonfly (uEye) camera uses the known features in $\{G_1\}$ ($\{G_2\}$) to compute its ego-motion. The Dragonfly (uEye) measures the distance and bearing to the uEye (Dragonfly) by detecting the ping-pong ball $\{B_2\}$ ($\{B_1\}$).

XII. Experimental Results

In this section, we describe a real-world experiment performed to further validate our extrinsic calibration algorithms. In the experiment, we use a Point Grey Dragonfly camera and an IDS uEye camera to mimic two robots moving in 3D (see Fig. 7). The two cameras are moved by hand such that they face each other and at the same time observe point features on a board placed behind each camera. These features are used to compute the cameras' ego-motion. Specifically, as depicted in Fig. 8, $\{C_1\}$ and $\{C_2\}$ denote the frames of reference for the Dragonfly and the uEye cameras, respectively. The pose of $\{C_1\}$ ($\{C_2\}$) in the global frame of reference $\{G_1\}$ ($\{G_2\}$) is determined by tracking features with known 3D coordinates in frame $\{G_1\}$ ($\{G_2\}$). In particular, we employ the direct least-squares solution for the PnP problem [32] to solve the camera pose given the image coordinates of known 3D points. After the pose of each camera in its global frame of reference is known, its transformation with respect to its initial frame (i.e., the quantities ${}^1\mathbf{p}_{2i+1}, {}^1_{2i+1}\mathbf{C}$, and ${}^2\mathbf{p}_{2i+2}, {}^2_{2i+2}\mathbf{C}$, $i = 1, \ldots, 4$) is easily obtained.

TABLE II
MINIMAL SYSTEMS' ESTIMATION ERRORS COMPARED TO THE LEAST-SQUARES SOLUTION

	Translation $\mathbf{p}$	Quaternion $\bar{q}$	$\|\|\delta\mathbf{p}\|\|$ (m)	$\|\|\delta\boldsymbol{\theta}\|\|$ (rad)
LS	-0.1618, 0.0864, 0.5122	-0.0923, -0.9744, 0.0900, 0.1841	0	0
sys1	-0.1465, 0.1198, 0.5795	-0.4776, -0.8581, 0.0148, 0.1878	0.0766	0.4008
sys2	-0.1491, 0.1219, 0.5897	-0.0885, -0.9818, 0.0626, 0.1558	0.0862	0.0402
sys5	-0.1282, 0.1048, 0.5070	-0.1225, -0.9778, 0.0589, 0.1596	0.0387	0.0499
sys6	-0.1465, 0.1198, 0.5795	-0.1948, -0.9805, 0.0255, 0.0084	0.0766	0.135
sys7	-0.1465, 0.1198, 0.5795	-0.0706, -0.9937, 0.0409, 0.0774	0.0766	0.1207

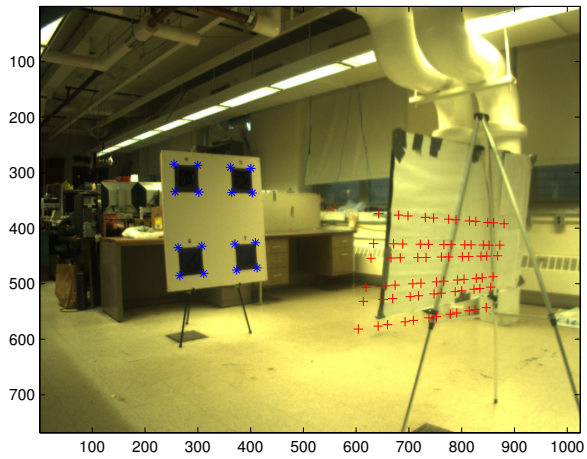

(a) Initial solution of System 2

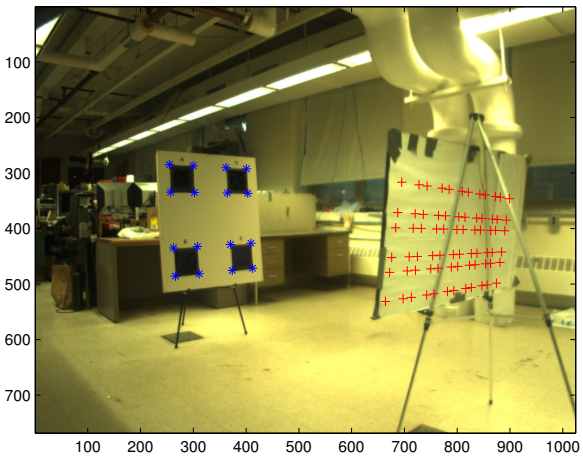

(b) Solution of System 2 after least-squares refinement

Fig. 9. Reprojected 3D feature points. The blue stars "*" are the back-projections of features in $\{G_1\}$. The red crosses "+" are the back-projections of features in $\{G_2\}$ which are expressed in frame $\{G_1\}$ using the estimated robot-to-robot transformation from: (a) the minimal solution of System 2; (b) the least-squares solution of System 2 initialized using the solution to the corresponding minimal problem.

The robot-to-robot distance and bearing measurements are obtained from images of the ping-pong ball mounted on top of each camera. Specifically, we first extract the edges of the ping-pong ball using the Canny edge detector [33]. Then, we fit a circle to the edge pixels using least squares. From the center and radius of the circle, we can measure both the bearing and range to the center of the ball from the camera, because the radius of the ball is known to be 20 mm. Finally, given the transformation between the camera $\{C_1\}$ to the ball $\{B_1\}$, and $\{C_2\}$ to $\{B_2\}$, we can compute the range and bearing between the two cameras. Therefore, we have both range and two bearings at all time steps, which allows us to pick and choose any measurement combination necessary for evaluating our extrinsic calibration algorithms.

Due to lighting conditions and motion blur, there are outliers in the ego-motion and robot-to-robot measurements. We perform RANSAC to eliminate outliers using the solutions of System 2 as hypothesis generator. We then refine the solution of the minimal System 2 using all the inliers by employing a least-squares algorithm, after which the accuracy of the robot-to-robot transformation is significantly improved.

To visualize the accuracy of the robot-to-robot relative pose estimates, we transform point features expressed in the global frame $\{G_2\}$ into $\{G_1\}$ using the estimated robot-to-robot transformation and the poses of the two cameras in their respective global frames. Then, we project all 3D features back onto a test image that has both feature boards in its field of view (see Fig. 9). Note that in this image, we can only see the front of the board with the 4 black squares, while the one with the 18 squares is facing in the opposite direction. The camera pose of this image is determined by using the 16 corner features of the 4 black squares. The reprojection of these 16 features (reflecting the accuracy of the PnP solution) are marked by blue stars, and the reprojection of the 4×18 features (reflecting the accuracy of the estimated robot-to-robot transformation) on the other board are marked by red crosses. We can see that the blue stars are at the corners of the 4 square targets, so the camera pose is very accurate. However, the red crosses in Fig. 9(a) are not precisely reprojected onto the white board. This is because the initial solution of System 2 has large errors in the robot-to-robot transformation. The robot-to-robot transformation becomes significantly more accurate after a least-squares refinement. In Fig. 9(b), the red crosses are all on the white board, although they are slightly shifted to the left.

Since the least-squares solution is the most accurate estimate of the robot-to-robot transformation, we use it as ground truth to assess the accuracy of the the minimal solutions of Systems 1–2 and 5–7. The computed estimates and the corresponding error norms are shown in Table II, where $\mathbf{p}$ denotes the relative translation, $\bar{q}$ is the quaternion corresponding to the relative rotation. $||\delta\mathbf{p}||$ is the 2-norm of the relative position error, and $||\delta\boldsymbol{\theta}||$ is the relative orientation error, both comparing

to the least-square solution (LS). The systems with mostly bearing measurements (Systems 2 and 5) appear to have the highest orientation accuracy. The orientation error of System 1 is particularly large (0.4008 rad). This is mainly due to the error in the robot-to-robot distance measurements. Finally, we should note that as in the simulation results, System 2 is the most resilient to measurement noise.

XIII. Conclusion and future Work

In this paper, we address the problem of computing relative robot-to-robot 3D translation and rotation using any combination of inter-robot measurements and robot ego-motion estimates. We have shown that there exist 14 base minimal systems which result from all possible combinations of inter-robot measurements. Except the two singular cases, Systems 3 and 4, we presented closed-form (algebraic) and analytical solutions to the remaining ones (see Fig. 2). A key advantage of the described methods is that they are significantly faster than other pure numerical approaches, such as homotopy continuation [30], since they require no iterations. Moreover, they can be used in conjunction with RANSAC for outlier rejection and for computing an initial estimate for the unknown robot-to-robot 3D transformation, which can be later refined using nonlinear least squares.

As future work, we plan to optimize the robots' motions such that the uncertainty in the robot-to-robot transformation is minimized. In particular, we will seek to determine the sequence of locations where the robots should move to so as to collect the most informative measurements, and thus achieve the desired level of accuracy in minimum time.

Appendix

A. Supplemental derivations for Systems 8, 9, and 10

In what follows, we show that in equation (91), $\mathbf{C}(\mathbf{u}_1, \theta) = \mathbf{C}(\mathbf{u}_1, 180^\circ)$. Using the Rodrigues formula for $\mathbf{C}(\mathbf{v}_1, 180^\circ)$, we have

$$\begin{aligned}\mathbf{C}(\mathbf{u}_1, \theta) &= \mathbf{C}_1^T \mathbf{C}(\mathbf{v}_1, 180^\circ)\mathbf{C}_2 \\ &= \mathbf{C}(\mathbf{e}_2, \beta_1 - \beta_2)^T(-\mathbf{I} + 2\mathbf{v}_1\mathbf{v}_1^T)\mathbf{C}(\mathbf{e}_2, \beta_1 + \beta_2)\end{aligned}$$

Substituting $\mathbf{v}_1 = \mathbf{C}(\mathbf{e}_2, \beta_1)\mathbf{u}_1$ (see Fig. 5) in the above equation, we have

$$\begin{aligned}\mathbf{C}(\mathbf{u}_1, \theta) &= -\mathbf{C}(\mathbf{e}_2, 2\beta_2) + 2\mathbf{C}(\mathbf{e}_2, \beta_2)\mathbf{u}_1\mathbf{u}_1^T\mathbf{C}(\mathbf{e}_2, \beta_2) \\ &= \mathbf{C}(\mathbf{e}_2, \beta_2)(-\mathbf{I} + 2\mathbf{u}_1\mathbf{u}_1^T)\mathbf{C}(\mathbf{e}_2, \beta_2) \\ &= \mathbf{C}(\mathbf{e}_2, \beta_2)\mathbf{C}(\mathbf{u}_1, 180^\circ)\mathbf{C}(\mathbf{e}_2, \beta_2) \\ &= \mathbf{C}(\mathbf{e}_2, \beta_2)\mathbf{C}(\mathbf{u}_1, 180^\circ)\mathbf{C}(\mathbf{e}_2, \beta_2)\mathbf{C}(\mathbf{u}_1, -180^\circ) \\ &\quad \cdot \mathbf{C}(\mathbf{u}_1, 180^\circ) \qquad (113) \\ &= \mathbf{C}(\mathbf{e}_2, \beta_2)\mathbf{C}(\mathbf{C}(\mathbf{u}_1, 180^\circ)\mathbf{e}_2, \beta_2)\mathbf{C}(\mathbf{u}_1, 180^\circ) \qquad (114) \\ &= \mathbf{C}(\mathbf{e}_2, \beta_2)\mathbf{C}(-\mathbf{e}_2, \beta_2)\mathbf{C}(\mathbf{u}_1, 180^\circ) \\ &= \mathbf{C}(\mathbf{u}_1, 180^\circ)\end{aligned}$$

where from (113) to (114) we have used the relation

$$\mathbf{C}(\mathbf{u}_1, 180^\circ)\mathbf{C}(\mathbf{e}_2, \beta_2)\mathbf{C}(\mathbf{u}_1, -180^\circ) = \mathbf{C}(\mathbf{C}(\mathbf{u}_1, 180^\circ)\mathbf{e}_2, \beta_2).$$

Hence, $\theta = 180^\circ$.

B. Summary of the 14 Systems

A summary of the problem formulation and solutions are listed in Table III.

References

[1] H. Sugiyama, T. Tsujioka, and M. Murata, "Coordination of rescue robots for real-time exploration over disaster areas," in *Proceedings of the* 11^{th} *IEEE International Symposium on Object Oriented Real-Time Distributed Computing (ISORC)*, Orlando, FL, May 5–7, 2008, pp. 170–177.

[2] M. Mazo Jr, A. Speranzon, K. H. Johansson, and X. Hu, "Multi-robot tracking of a moving object using directional sensors," in *Proceedings of the IEEE International Conference on Robotics and Automation*, New Orleans, LA, Apr. 26–May 1, 2004, pp. 1103–1108.

[3] S. I. Roumeliotis and G. A. Bekey, "Distributed multirobot localization," *IEEE Transactions on Robotics and Automation*, vol. 18, no. 5, pp. 781–795, Oct. 2002.

[4] R. Madhavan, K. Fregene, and L. E. Parker, "Distributed cooperative outdoor multirobot localization and mapping," *Autonomous Robots*, vol. 17, no. 1, pp. 23–39, Jul. 2004.

[5] L. Doherty, K. S. J. Pister, and L. E. Ghaoui, "Convex position estimation in wireless sensor networks," in *Proceedings of INFOCOM* 20^{th} *Annual Joint Conference of IEEE Computer and Communications Society*, Anchorage, AK, Apr. 22–26, 2001, pp. 1655–1663.

[6] Y. Shang, W. Ruml, Y. Zhang, and M. P. J. Fromherz, "Localization from mere connectivity," in *Proceedings of the* 4^{th} *ACM International Symposium on Mobile Ad Hoc Networking and Computing*, Annapolis, MD, Jun. 1–3, 2003, pp. 201–212.

[7] X. S. Zhou and S. I. Roumeliotis, "Determining the robot-to-robot 3D relative pose using combinations of range and bearing measurements: 14 minimal problems and closed-form solutions to three of them," in *Proceedings of the IEEE/RSJ International Conference on Intelligent Robots and Systems*, Taipei, Taiwan, Oct. 18–22, 2010, pp. 2983 – 2990.

[8] ——, "Determining the robot-to-robot 3D relative pose using combinations of range and bearing measurements (part II)," in *Proceedings of the IEEE International Conference on Robotics and Automation*, Shanghai, China, May 9–13, 2011, pp. 4736–4743.

[9] M. Fischler and R. Bolles, "Random sample consensus: A paradigm for model fitting with application to image analysis and automated cartography," *Communications of the ACM*, vol. 24, no. 6, pp. 381–395, Jun. 1981.

[10] J. Aspnes, T. Eren, D. K. Goldenberg, A. S. Morse, W. Whiteley, Y. R. Yang, B. D. O. Anderson, and P. N. Belhumeur, "A theory of network localization," *IEEE Transactions on Mobile Computing*, vol. 5, no. 12, pp. 1663–1678, Dec. 2006.

[11] T. Eren, D. K. Goldenberg, W. Whiteley, Y. R. Yang, A. S. Morse, B. D. O. Anderson, and P. N. Belhumeur, "Rigidity, computation, and randomization in network localization," in *Proceedings of INFOCOM* 23^{rd} *Annual Joint Conference of the IEEE Computer and Communications Societies*, Hong Kong, Mar. 7–11, 2004, pp. 2673–2684.

[12] J. Nie, "Sum of squares method for sensor network localization," *Computational Optimization and Applications*, vol. 43, no. 2, pp. 1573–2894, Jun. 2009.

[13] C.-H. Ou and K.-F. Ssu, "Sensor position determination with flying anchors in three-dimensional wireless sensor networks," *IEEE Transactions on Mobile Computing*, vol. 7, no. 9, pp. 1084–1097, Sep. 2008.

[14] S. Higo, T. Yoshimitsu, and I. Nakatani, "Localization on small body surface by radio ranging," in *Proceedings of the 16th AAS/AIAA Space Flight Mechanics Conference*, Tampa, FL, Jan. 22–26, 2006.

[15] Y. Dieudonné, O. Labbani-Igbida, and F. Petit, "Deterministic robot-network localization is hard," *IEEE Transactions on Robotics*, vol. 26, no. 2, pp. 331–339, Apr. 2010.

[16] A. Martinelli and R. Siegwart, "Observability analysis for mobile robot localization," in *Proceedings of the IEEE/RSJ International Conference on Intelligent Robots and Systems*, Edmonton, Canada, Aug. 2–6, 2005, pp. 1471–1476.

[17] X. S. Zhou and S. I. Roumeliotis, "Multi-robot SLAM with unknown initial correspondence: The robot rendezvous case," in *Proceedings of the IEEE/RSJ International Conference on Intelligent Robots and Systems*, Beijing, China, Oct. 9–15, 2006, pp. 1785–1792.

[18] A. Howard, L. E. Parker, and G. S. Sukhatme, "Experiments with a large heterogeneous mobile robot team: Exploration, mapping, deployment and detection," *International Journal of Robotics Research*, vol. 25, no. 5–6, pp. 431–447, May 2006.

TABLE III
SOLUTION SUMMARY

Sys.	Measurements	System Equations	Parameterization	Solution
1	$d_{12}, \mathbf{b}_1; \mathbf{b}_2, d_{34}$	$\mathbf{b}_1 + \mathbf{C}\mathbf{b}_2 = \mathbf{0}$ $\mathbf{v}^T\mathbf{C}^2\mathbf{p}_4 + a = 0$	$\mathbf{C} = \mathbf{C}(-\mathbf{b}_1, \alpha)\mathbf{C}(\mathbf{w}, \beta)$ $\mathbf{w} = \frac{\mathbf{b}_1 \times \mathbf{b}_2}{\|\mathbf{b}_1 \times \mathbf{b}_2\|}$	$\beta = Atan2(\|\|\mathbf{b}_1 \times \mathbf{b}_2\|\|, -\mathbf{b}_1^T\mathbf{b}_2)$ α = 2 solutions from (26) and (27) $\mathbf{p} = d_{12}\mathbf{b}_1$
2	$\mathbf{b}_1, \mathbf{b}_2; \mathbf{b}_3$	$\mathbf{b}_1 + \mathbf{C}\mathbf{b}_2 = \mathbf{0}$ $\mathbf{v}^T\mathbf{C}^2\mathbf{p}_4 + a = 0$ $d_{12} = \frac{(\lfloor \mathbf{b}_3 \times \rfloor \mathbf{b}_1)^T \lfloor \mathbf{b}_3 \times \rfloor ({}^1\mathbf{p}_3 - \mathbf{C}^2\mathbf{p}_4)}{(\lfloor \mathbf{b}_3 \times \rfloor \mathbf{b}_1)^T (\lfloor \mathbf{b}_3 \times \rfloor \mathbf{b}_1)}$		
3	$d_{12}, \mathbf{b}_1; d_{34}, \mathbf{b}_3$	$(\mathbf{p} - d_{34}\mathbf{b}_3 - {}^1\mathbf{p}_3) + \mathbf{C}^2\mathbf{p}_4 = 0$		Infinite solutions for $\mathbf{C}$ $\mathbf{p} = d_{12}\mathbf{b}_1$
4	$d_{12}, \mathbf{b}_1; d_{34}, \mathbf{b}_4$	$\mathbf{p} - {}^1\mathbf{p}_3 + \mathbf{C}({}^2\mathbf{p}_4 + d_{34}\mathbf{b}_4) = 0$		
5	$\mathbf{b}_1$, $\mathbf{b}_2$; d_{34}; d_{56}	$\mathbf{b}_1 + \mathbf{C}\mathbf{b}_2 = \mathbf{0}$ $d_{12}^2 + 2d_{12}(\mathbf{b}_1^T\mathbf{C}^2\mathbf{p}_4 - \mathbf{b}_1^T{}^1\mathbf{p}_3) - 2 \cdot {}^1\mathbf{p}_3^T\mathbf{C}^2\mathbf{p}_4 + \epsilon_1 = 0$ $d_{12}^2 + 2d_{12}(\mathbf{b}_1^T\mathbf{C}^2\mathbf{p}_6 - \mathbf{b}_1^T{}^1\mathbf{p}_5) - 2 \cdot {}^1\mathbf{p}_5^T\mathbf{C}^2\mathbf{p}_6 + \epsilon_2 = 0$	$\mathbf{C} = \mathbf{C}(-\mathbf{b}_1, \alpha)\mathbf{C}(\mathbf{w}, \beta)$ $\mathbf{w} = \frac{\mathbf{b}_1 \times \mathbf{b}_2}{\|\mathbf{b}_1 \times \mathbf{b}_2\|}$	$\beta = Atan2(\|\|\mathbf{b}_1 \times \mathbf{b}_2\|\|, -\mathbf{b}_1^T\mathbf{b}_2)$ d_{12} = 4 solutions from (39) α = 4 solutions from (37) $\mathbf{p} = d_{12}\mathbf{b}_1$
6	d_{12}, $\mathbf{b}_1$; $\mathbf{b}_3$; d_{56}	$\lfloor \mathbf{b}_3 \times \rfloor \mathbf{u} = \lfloor \mathbf{b}_3 \times \rfloor \mathbf{C}\mathbf{v}$ $\mathbf{u}'^T\mathbf{C}\mathbf{v}' + a = 0$		$\mathbf{C}$ = 2 solutions from Σ_1 and 2 solutions from Σ_2 in (59) $\mathbf{p} = d_{12}\mathbf{b}_1$
7	d_{12}, $\mathbf{b}_1$; $\mathbf{b}_4$; d_{56}			
8	$\mathbf{b}_1$; $\mathbf{b}_3$; $\mathbf{b}_5$	$\mathbf{v}_1^T\mathbf{C}\mathbf{u}_1 - w_1 = 0$ $\sum \mathbf{v}_i^T\mathbf{C}\mathbf{u}_i - w_i = 0$, i = 2, 3	$\mathbf{C} = \mathbf{C}(\mathbf{v}_1, \alpha)\mathbf{C}(\mathbf{e}_2, \beta)\mathbf{C}(\mathbf{u}_1, \gamma)$ $\mathbf{e}_2 = \frac{\mathbf{u}_1 \times \mathbf{v}_1}{\|\mathbf{u}_1 \times \mathbf{v}_1\|}$	$\beta = \arccos(\mathbf{u}_1^T\mathbf{v}_1) - \arccos(w_1)$ 8 solutions for α and γ from (88) (86)
9	$\mathbf{b}_1$; $\mathbf{b}_3$; $\mathbf{b}_6$			
10	d_{12}, $\mathbf{b}_1$; d_{34}; d_{56}; d_{78}			
11	$\mathbf{b}_1$; $\mathbf{b}_3$; d_{56}; d_{78}	$\|\|\mathbf{p} + \mathbf{C}^2\mathbf{p}_6 - {}^1\mathbf{p}_5\|\|^2 = d_{56}^2$ $\|\|\mathbf{p} + \mathbf{C}^2\mathbf{p}_8 - {}^1\mathbf{p}_7\|\|^2 = d_{78}^2$ $\mathbf{v}_2^T\mathbf{C}^2\mathbf{p}_4 - \mathbf{v}_2^T{}^1\mathbf{p}_3 = 0$ $d_{12} = \mathbf{v}_1^T\mathbf{C}^2\mathbf{p}_4 + a$	$\mathbf{C} = \mathbf{I}_3 - 2q_4\lfloor \mathbf{q} \times \rfloor + 2\lfloor \mathbf{q} \times \rfloor^2$	Employ Reid and Zhi's multiplication matrix method [28].
12	$\mathbf{b}_1$; $\mathbf{b}_4$; d_{56}; d_{78}	$d_{12}\mathbf{v}_i^T\mathbf{C}^T\mathbf{b}_1 - \mathbf{v}_i^T\mathbf{C}^T{}^1\mathbf{p}_3 + \mathbf{v}_i^T{}^2\mathbf{p}_4 = 0$, $i = 1, 2$ $\|\|d_{12}\mathbf{b}_1 + \mathbf{C}^2\mathbf{p}_6 - {}^1\mathbf{p}_5\|\|^2 = d_{56}^2$ $\|\|d_{12}\mathbf{b}_1 + \mathbf{C}^2\mathbf{p}_8 - {}^1\mathbf{p}_7\|\|^2 = d_{78}^2$		
13	$\mathbf{b}_1$; d_{34}; d_{56}; d_{78}; $d_{9,10}$	$\|\|d_{12}\mathbf{b}_1 + \mathbf{C}^2\mathbf{p}_4 - {}^1\mathbf{p}_3\|\|^2 = d_{34}^2$ $\|\|d_{12}\mathbf{b}_1 + \mathbf{C}^2\mathbf{p}_6 - {}^1\mathbf{p}_5\|\|^2 = d_{56}^2$ $\|\|d_{12}\mathbf{b}_1 + \mathbf{C}^2\mathbf{p}_8 - {}^1\mathbf{p}_7\|\|^2 = d_{78}^2$ $\|\|d_{12}\mathbf{b}_1 + \mathbf{C}^2\mathbf{p}_{10} - {}^1\mathbf{p}_9\|\|^2 = d_{9,10}^2$		

[19] X. S. Zhou and S. I. Roumeliotis, "Robot-to-robot relative pose estimation from range measurements," *IEEE Transactions on Robotics*, vol. 24, no. 6, pp. 1379–1393, Dec. 2008.

[20] C. W. Wampler, "Forward displacement analysis of general six-in-parallel SPS (Stewart) platform manipulators using soma coordinates," *Mechanism and Machine Theory*, vol. 31, no. 3, pp. 331–337, Apr. 1996.

[21] T.-Y. Lee and J.-K. Shim, "Improved dialytic elimination algorithm for the forward kinematics of the general Stewart-Gough platform," *Mechanism and Machine Theory*, vol. 38, no. 6, pp. 563–577, Jun. 2003.

[22] N. Trawny, X. S. Zhou, and S. I. Roumeliotis, "3D relative pose estimation from six distances," in *Proceedings of Robotics: Science and Systems*, Seattle, WA, Jun. 28 – Jul. 1, 2009, pp. 233–240.

[23] D. Stewart, "A platform with six degrees of freedom: A new form of mechanical linkage which enables a platform to move simultaneously in all six degrees of freedom developed by elliott-automation," *Aircraft Engineering and Aerospace Technology*, vol. 38, no. 4, pp. 30–35, 1993.

[24] N. Trawny, X. S. Zhou, K. X. Zhou, and S. I. Roumeliotis, "Interrobot transformations in 3D," *IEEE Transactions on Robotics*, vol. 26, no. 2, pp. 225–243, Apr. 2010.

[25] I. Stewart, *Galois Theory*, 3rd ed. Chapman and Hall/CRC Mathematics Series, 2003.

[26] D. A. Cox, J. Little, and D. O'Shea, *Using Algebraic Geometry*, 2nd ed. Springer, 2004.

[27] X. S. Zhou and S. I. Roumeliotis, "Determining the robot-to-robot relative pose using range and/or bearing measurements," University of Minnesota, Dept. of Comp. Sci. & Eng., MARS Lab, Tech. Rep., Feb. 2010. [Online]. Available: www.cs.umn.edu/~zhou/paper/14systech.pdf

[28] G. Reid and L. Zhi, "Solving polynomial systems via symbolic-numeric reduction to geometric involutive form," *Journal of Symbolic Computation*, vol. 44, no. 3, pp. 280–291, Mar. 2009.

[29] X. S. Zhou, "Motion induced robot-to-robot extrinsic calibration," Ph.D. dissertation, University of Minnesota, May 2012. [Online]. Available: http://www-users.cs.umn.edu/~zhou/paper/ZhouPhDthesis.pdf

[30] J. Verschelde, "Algorithm 795: PHCpack: A general-purpose solver for polynomial systems by homotopy continuation," *ACM Transactions on Mathematical Software*, vol. 25, no. 2, pp. 251–276, 1999.

[31] N. Trawny and S. I. Roumeliotis, "Indirect Kalman filter for 3D attitude estimation," University of Minnesota, Dept. of Comp. Sci. & Eng., Tech. Rep. 2005-002, Jan. 2005.

[32] J. A. Hesch and S. I. Roumeliotis, "A direct least-squares (DLS) solution for PnP," in *Proceedings of the International Conference on Computer Vision*, Barcelona, Spain, Nov. 6–13, 2011, pp. 383–390.

[33] J. F. Canny, "A computational approach to edge detection," *IEEE Transactions on Pattern Analysis and Machine Intelligence*, vol. 6, pp. 679–698, 1986.

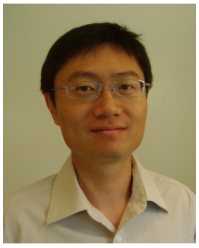

Xun S. Zhou received his B.Sc. in Physics with honors from the Zhongshan University, China in 2000, the M.Sc. in Computer Science from the Bradley University, IL in 2003, and Ph.D in Computer Science from University of Minnesota, MN in 2012. He is currently a Computer Scientist at SRI International Sarnoff, NJ. His research interests lie in the areas of single- and multi-robot systems, localization and mapping, multi-sensor extrinsic calibration, and computer vision. He is the recipient of the 2007 Excellence in Research Award from the CSE Department of the University of Minnesota, and in 2006 he was the Finalist for the Best Paper Award of the IEEE/RSJ International Conference on Intelligent Robots and Systems.

Stergios I. Roumeliotis received the Diploma in Electrical Engineering from the National Technical University of Athens, Greece, in 1995, and the M.S. and Ph.D. degrees in Electrical Engineering from the University of Southern California, CA in 1999 and 2000 respectively. From 2000 to 2002 he was a Postdoctoral Fellow at the California Institute of Technology, CA. Between 2002 and 2008 he was an Assistant Professor with the Department of Computer Science and Engineering, University of Minnesota, MN, where he is currently an Associate Professor. Since 2009, S.I. Roumeliotis is the Associate Director for Research of the Digital Technology Center (DTC). His research interests include vision-aided inertial navigation of aerial and ground autonomous vehicles, distributed estimation under communication and processing constraints, and active sensing for reconfigurable networks of mobile sensors.

S.I. Roumeliotis is the recipient of the Guillermo E. Borja Award (2009), the National Science Foundation (NSF) Presidential Early Career Award for Scientists and Engineers (PECASE) (2008), the NSF CAREER award (2006), the McKnight Land-Grant Professorship award (2006-08), the ICRA Best Reviewer Award (2006), and he is the co-recipient of the One NASA Peer award (2006), and the One NASA Center Best award (2006). Papers he has co-authored have received the King-Sun Fu Best Paper Award of the IEEE Transactions on Robotics (2009), the Robotics Society of Japan Best Journal Paper award (2007), the ICASSP Best Student Paper award (2006), the NASA Tech Briefs award (2004), and three of them were Finalists for the RSS Best Paper Award (2009), the ICRA Best Student Paper Award (2009) and the IROS Best Paper Award (2006). S.I. Roumeliotis served as Associate Editor for the IEEE Transactions on Robotics between 2006 and 2010.

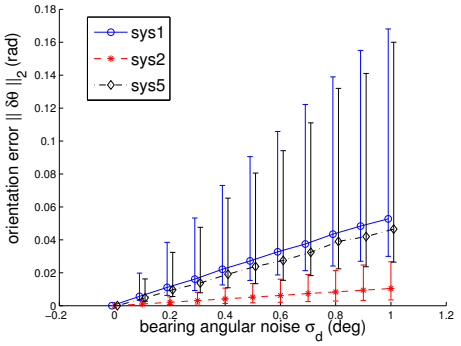

(a) Sys 1, 2, and 5: Orientation error

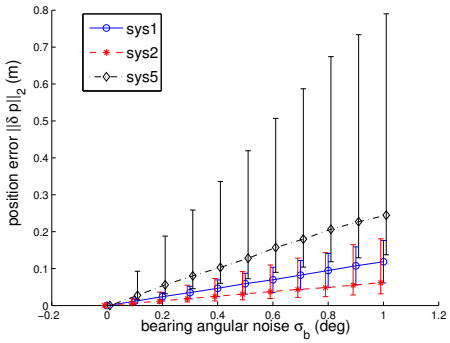

(b) Sys 1, 2, and 5: Position error

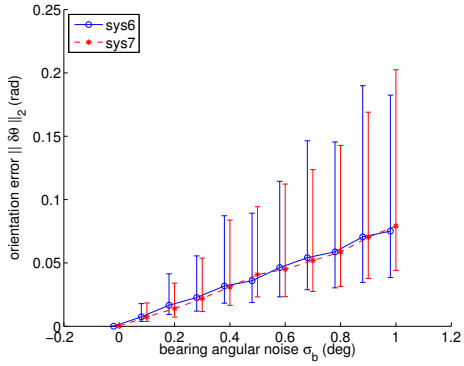

(c) Sys 6 and 7: Orientation error

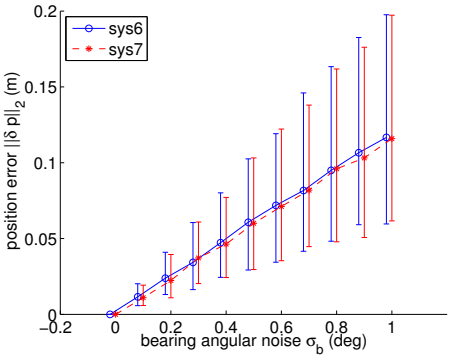

(d) Sys 6 and 7: Position error

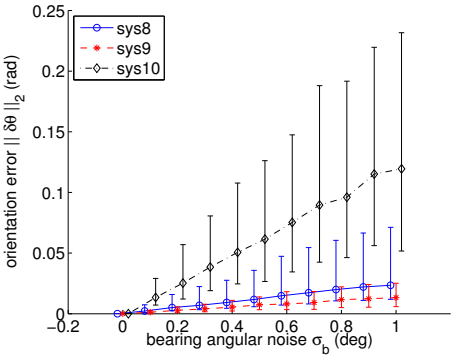

(e) Sys 8, 9, and 10: Orientation error

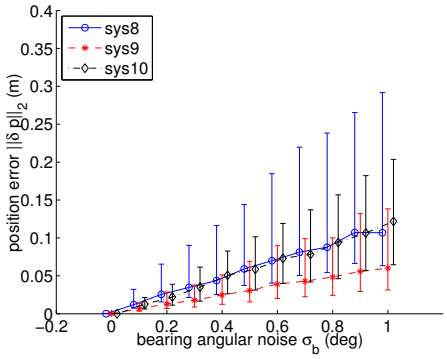

(f) Sys 8, 9, and 10: Position error

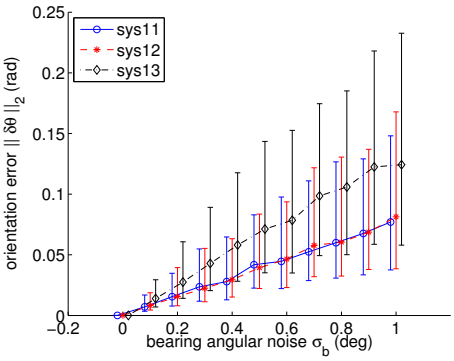

(g) Sys 11, 12 and 13: Orientation error

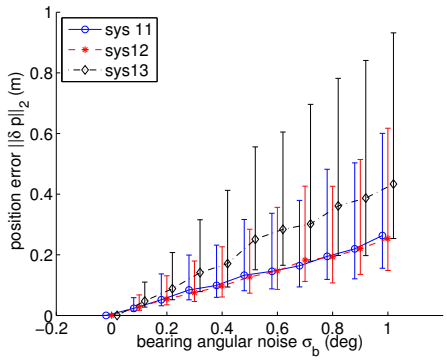

(h) Sys 11, 12, and 13: Position error

Fig. 6. Orientation and position errors as functions of the bearing-measurement noise. The plots show the median and 25–75% quartiles in 1000 trials.